NTNU

Norwegian University of
Science and Technology

Experimental study of the airflow distribution in a room with heating equipment

Joanna Polak

Master's Thesis
Submission date: September 2015
Supervisor: Guangyu Cao, EPT

Norwegian University of Science and Technology
Department of Energy and Process Engineering

PREFACE

This report represents my Master Thesis and was prepared at Department of Energy and Process Engineering at the Norwegian University of Science and Technology in Trondheim, Norway. All of experimental works in the study were done in the Energy and Indoor Environment Laboratory.

I would like to thank my supervisor professor Guangyu Cao for his help and guidance, patience and sacrificed time.

I wish to thank my co-supervisors Laurent Georges, Øyvind Skreiberg and all people who help me while preparing the measurements place in the lab.

I also want to thank my fellow master student Aleksandra Szopa for her help in the lab, for her support and for all shared discussion during the experimental period.

Joanna Polak,

Katowice, September 2015

SUMMARY

Energy consumption in building sector has led to a great need for energy saving and energy efficient solutions for buildings. Next generation of buildings should apply high energy performance solutions in order to decrease the energy consumption. The Energy Performance of Buildings Directive (EPBD) requires that by the end of 2020 all new buildings should be nearly Zero Energy Buildings (nZEB). Therefore the tremendous efforts and emphasis have been put on development of new feasible solutions. Reducing the energy needs in nZEBs may lead to simplification of space heating system. With a long tradition and environmental friendly aspects, using wood stoves encourage their integration in nZEB. Recent investigation assume the one wood stove may ensure thermal comfort in the whole dwelling if the internal doors are open. However, it still remains unclear due to lack of understanding of some fundamental aspects, including heat transfer within or between different zones, temperature stratification inside zones, accumulation of particles in a certain zone in the building. The goal of this project work is to characterize the airflow distribution in a room with an air curtain and an additional heating equipment. Experimental measurements were performed in a full-scale climate chamber at NTNU Norwegian University of Science and Technology. The results of the experimental measurements are presented in this thesis to show the temperature and velocity distribution in the room, which contains two zones with temperature differences. This thesis assume better heat distribution through optimum passive and active methods. Therefore the effect of distributing the warm air through the slot diffuser generating downward plane jet has been investigated. The diffuser was installed above the doorway between warm and cold zones. Different discharged velocities from the diffuser were used during experiment. Additionally the influence of different heat source type and different heat source locations were investigated. The results showed that installing of the air curtain system between zones may decrease vertical temperature stratification and increase rapid of heat distribution between zones. Discharged velocities directly affect the performance of the airflow distribution between zones. Supplying the warm air through the air curtain system installed above the doorway may lead to reduction of the vertical temperature stratification inside both zones of the doorway. In addition, the investigation showed that the type of the heat source seems to not have a significant impact on the airflow distribution while using the air curtain system.

NOMENCLATURE

Latin symbols:

A_c	slot area, m^2
b	half width of the jet, m,
C_b	constant for a given angle, -
d_N	diameter of the slot, m
g	acceleration due to gravity, m/s^2
h	height of the aperture, m
$\dot{J}$	momentum flux, N,
K	dynamic coefficient of the jet, -
l	length of the jet, m
$\dot{m}$	mass flow, kg/s,
M_0	initial momentum flux, $kg \cdot m^2/s$
p	pressure, Pa
q_0	volume discharged from the slot, m^3/h
q_{entr}	volume of the ambient air entering the jet, m^3/h
t	time, s
u	air velocity, m/s,
u_0	outlet velocity discharged from the slot, m/s
u_{max}	maximum air velocity
$\dot{V}$	volume flow, m^3/s,
x	distance downstream of the jet slot, m

Greek symbols:

α	widening angle (20-30°)
ρ	air density, kg/m^3

TABLE OF CONTENTS

1. Introduction

1.1. Problem statement

During the last decades great emphasis was put on reduction of energy consumption in building sector. In a European perspective the building sector states for 24.6% of the final energy consumption (Eurostat, 2006-2007). Accordingly to International Energy Agency (IEA), in terms of primary energy consumption, buildings represent even 40%. Therefore the idea of creating buildings that have a very high energy performance became crucial.

There is no single definition of nearly Zero Energy Buildings (nZEB) but one is universal that those are buildings that has a very high energy performance. The Energy Performance of Buildings Directive presents the following sentence regarding nZEB: "The nearly zero or very low amount of energy required should be covered to a very significant extent by energy from renewable sources, including energy from renewable sources produced on-site or nearby". Due to different climates and various building cultures in European countries creation of national definition of nZEB is required. Therefore there are many different national applications of the definition of nearly zero-energy buildings which require further examination.

Typically, low-energy buildings have highly-insulated envelope and very energy efficient windows. They are characterized by high level of air tightness. These features lead to decrease of energy used for heating. In consequence it can be assumed that it is no longer required to place heat emitter in each room of the building so the space-heating distribution system can therefore be simplified. Looking towards increasing usage of renewable energy resources, wood stoves appear as an attractive alternative for traditional heating systems. However there are still many issues which require detailed investigation e.g. the impact of the wood stoves on the indoor airflow quality and air distribution is unknown.

Although usage of wood stoves has a long tradition there are still many challenges on the way to integrate them with future buildings generation. Energy needs of nZEBs are too low comparing to power of wood stoves existing on the market. The question arises whether the high power of current stoves may lead to unacceptable overheating of the room where the stove is located. It remains unclear if one wood stove can efficiently heat up the whole building without a risk of neglecting thermal comfort of the occupants. Another issues such as long operation time of the stoves, heat and mass transfer within or between different zones or accumulation of particles in a certain zone in the building may have a significant impact of the wood stoves adaptation into high energy performance buildings.

Therefore the following questions need to be considered in order to investigate a possibility of applying wood stoves in nZEB:

- How to decrease the risk of overheating of the room in which additional heat source is located?
- What is the impact of heat source on the airflow distribution inside the building?
- How to improve heat distribution between zones?

These questions are the most relevant for the thesis. The research focus on the airflow distribution inside and between zones in the building equipped with only one space-heating device.

The possibility of heating a passive house with a single wood stove is defined by the following challenges:

- To investigate how a single heat source located in one thermal zone is able to mainly perform the space heating in a passive house.
- To investigate how an oversized wood stove can operate with long production cycles in a passive house without generating overheating.

- To investigate the resulting energy efficiency of a wood stove for the space heating distribution.

Another aim is to improve a range of stove properties i.e. nominal combustion power of the stove and the power modulation. One of the main outcome of recent research is that: 'the wood stove may cover a significant part of the heating load during a Typical Meteorological Year if the building occupants can accept a lower operative temperature in bedrooms and often leave the internal doors of the building open' (Georges et al. 2013).

The reducing space heating system can lead to temperature differences inside other rooms which remain unheated. In order to achieve a proper indoor thermal environment, the heat transfer between the rooms should be improved. The heat distribution between different zones is the objective of another research (Mathisen & Georges, 2015). The investigation presents results of measurements conducted in real passive house located in Trondheim, Norway. The rate of discharge through the staircase and the indoor environment parameters such as air temperature, air velocity and surface temperature of walls were analyzed. Different space heating emission subsystems were using during the experiment. The heating device was located in the living room and the rest of the passive house remains unheated. The results presents that 'the mass flow rate through the door is one order of magnitude higher than the nominal hygienic ventilation flow rates'.

1.2. Objective of this study

Considering state-of-the-art investigations and existing problems the following conception of this investigations has been created.

The goal of the project work is to characterize the airflow distribution between zones in a room with an additional heating equipment. An electric stove was used to mimic a wood stove to get better understanding of heat distribution of airflow distribution in nZEB while

using an additional heating device. The influence of an indoor heating device on the performance of the indoor airflow distribution was also studied by using different supplied airflow rate in a room. The heat distribution results from the airflow movement. Air temperature and air velocity are the two main parameters used in this thesis to describe airflow distribution and in consequence the heat distribution. Measurements results were obtained from the experimental conditions of the airflow distribution generated by the slot diffuser located above the doorway between two zones.

The main aim of the research is to improve indoor air distribution in building equipped with the wood stove. The investigation are focused on providing better heat transfer inside the building by combining heat and ventilation systems.

2. Heat distribution method in Zero Emissions Building

"Buildings are getting tighter and better insulated in order to reduce their energy needs caused by heat loss via transmission and uncontrolled air flows" (Kunkel & Kontonasiou). Ventilation, heating and cooling strategies need to be designed in order to maximize the efficiency of usage of renewable sources and thus limit the environmental impact. The required energy must be supplied utilizing the lowest cost and most environmentally-friendly energy sources possible (Mathisen & Georges, 2015). In order to ensure thermal comfort in the entire building, the heat transfer between rooms needs to be promoted.

2.1. Passive heat distribution solutions

Passive heat distribution considers methods which do not use any special systems to distribute the heat and do not charge electric power to cause heat transport. The air movement is caused by density gradient between warm and cold rooms. This is called gravitational flow. Different studies investigate bidirectional airflow through the large openings with regard to

airflow through the internal door openings. The investigation showed that the opening of internal doors is an efficient way to homogenize temperature in passive houses (Mathisen & Georges, 2015). In fact, a strong bidirectional flow will be generated through doorways with flow rates that are significantly higher than the nominal airflow rates provided by the balanced mechanical ventilation. However, there is still a lack of a measurement data which may confirms this.

The classical simplified methods of the gravitational flow apply the continuity equation and Bernoulli's theorem on both sides of the large opening. The dynamics of general fluid flow is based on the conservation of mass principle and the conservation of momentum principle. The only external force that is considered is gravity (International Energy Agency, 1992).

$$p = p_0 - g \int_0^z \rho \tag{1}$$

Where p is the local density which may vary due to differences in temperature between zones, z is height and g is the acceleration due to gravity.

The baseline case investigated during the experiment assumes that the heating system is not combined to any ventilation system. The first zone is equipped with the internal heating device and consider as a warm zone. The second zone remains unheated and in this thesis is referred to cold zone.

The door between zones are open. The air movement is caused only by density differences. The warm air stream floats upward and occupies upper part of the warm zone. After that heated air starts to escape warm zone through the doorway and enters the upper part of cold zone. At the same time the cold air stream inside the cold zone falls down and starts entering warm zone. Accordingly to the theory both streams should have the same masses. Theoretical velocity profile along the door opening is presented on *Figure 1*. The largest velocity values appear at the lowest and the highest levels of the aperture. Velocity decreased towards middle of the opening. In the middle of the orifice neutral plane is located. Neutral plane level h_n is

the height in the aperture where the pressure difference between the two zones is zero and therefore the velocity is also zero.

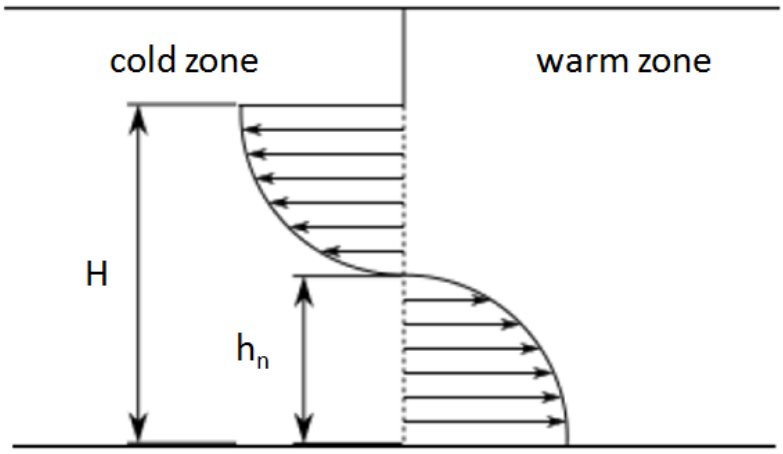

Figure 1. The airflow pattern along the door opening located between zones with temperature difference. H indicates the height of the aperture, h_n refers to the height where neutral plane is located (Pettersen, 2014).

There is no power supplied to force the airflow movement, therefore this can be called passive heat distribution method. *Figure 2* presents schematic airflow distribution in the room for the baseline case described above. In this case different types and different positions of the heat source were used (see *0.*

Experimental setup)

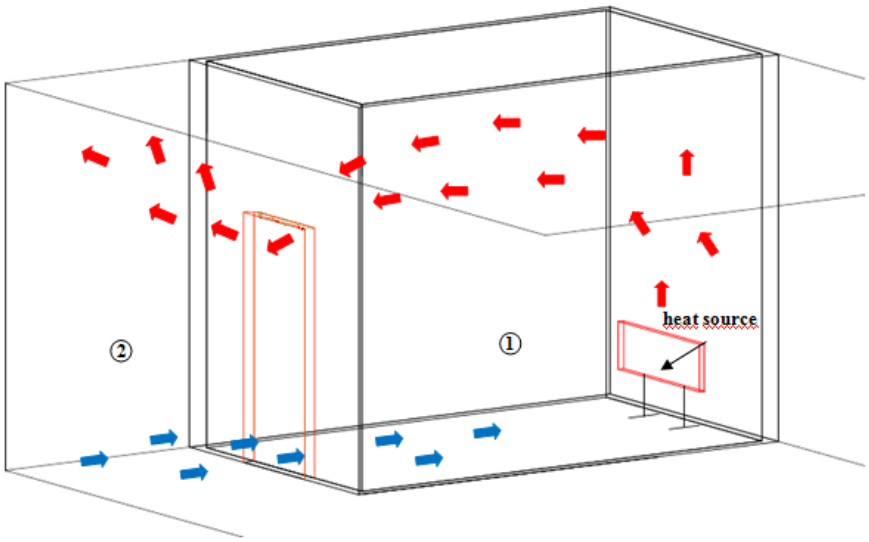

Figure 2. Schematic airflow distribution through the door opening between cold and warm zones.

However this basic case can lead to large temperature stratification inside zones. The huge amount of warm air remains concentrated in upper part of both zones. The process of mixing two streams, cold and warm, is time consuming. Thermal comfort cannot be obtained while the lower part of the room which contains also occupants zone stays cold. Big temperature differences between zones may cause high velocity values appearing in the vicinity of the doorway and the limit when the draught can be felt may be exceeded, especially at lower part of the zone.

Using wood stoves as the only heating source in building can be considered as the passive heat distribution method. "Wood stove is an up-to-date low-carbon technology and usually considered a low-carbon and low-cost renewable energy system based on local resources in the form of residual biomass from the local surroundings" (Carvalho, et al., 2013).

However there are many challenges while integrating the wood stove into the nearly Zero Energy Buildings. The growing efficiency of the wood stoves which can achieve even 85% and their environmental friendly aspects encourage scientist and companies to improve the features of wood stoves in order to unable the proper integration into the new generation of

buildings. ‘Stable Wood Stoves’, current project of SINTEF, which is one of the largest research organization in Scandinavia, analyze aspects connected to emissions, efficiencies and the transient heat release from combustion of wood logs in wood stove (Bugge, Skreiberg, Seljeskog, & Lundquist, 2014). The research project combine experimental work and simulations and contains combustion process and heat release of the wood stoves, the impact of the wood stove on an indoor air quality, an issue of emission and energy efficiency of the stoves.

Both the combustion process, heat release and the storage of the heat have to correspond to the current energy needs of the building. The important problem on the way to integration of the wood stove in nZEB is that current available wood stoves provide too large amount of power. The energy needs of the nZEBs decreased to 1 kW and these units do are not available on the market today. Therefore the aim to create ‘stable wood stoves’ becomes crucial. More stable heat release is the main focus when designing next generation of wood stoves.

Due to the low heat needs of nearly Zero Energy Buildings it is important to achieve a heat release profile without an excessive peak effect. Moreover integration of wood stoves to the low energy performance buildings also needs to ensure a proper indoor air quality. The requirements are limited by following parameters: emissions of particulate matter, organic gaseous compounds, carbon monoxide and nitrogen oxides. The airtight building envelopes combined with mechanical ventilation system require separated air systems for combustion air and flue gas evacuation. The wood stoves need be able to operate without the risks of indoor smoke leakage. However the emission into the room while operating of the wood stove is possible mostly in a start-up-phase and during refilling of the stove. Therefore the big challenge is to minimize these emissions to ensure an optimum indoor air quality.

Continuous activity connected to standardization of approval tests for wood stoves participated in international standardization work as wells a in the development and testing of

measurements methods to be introduced in updated standards. This will also be a requirement for future's wood stoves in low-energy and passive houses, as a means to achieve a higher operational flexibility for covering the heat demand at a wide range throughout the heating season.

2.2. Active heat distribution solutions

The active heat distribution methods consider using of special distributing circuit which require delivering of electrical energy i.e. to power the circulating pumps (or fans if it's air conditioning). Basically the main heating source is connected to heat distribution systems which bring heat to the local space heating devices. However heat distribution may be carried out through the building system integration. Building of tighter dwellings in the last decades has reduced the infiltration rates, and there has been a need for controlled ventilation to provide an acceptable indoor air quality. In low energy buildings the energy demand for space heating is very low and the use of a combination of ventilation and heating systems may be an interesting alternative to a separate heating system. Nevertheless convective flows due to buoyancy forces are likely to produce air flows larger than the mechanical ventilation supply rates in residential buildings.

There are many examples of active methods e.g. hydro pellet stoves which burn biomass and are equipped with a heat exchanger to produce hot water. In this case the main part of the combustion heat is recovered by this exchanger while the remaining is directly emitted into the room. The huge advantage is that the power released into the room is significantly decreased so that it prevents overheating and the generated hot water can be stored in a storage tank. Another available methods of distribution the warm air is to supply the warm air directly to the room. Active heat distribution methods consider also integration heat pomp systems and solar panels into the heating systems.

The next case in this study presents new active heat distribution method and assume heat and ventilation systems cooperation. The slot diffuser will be installed above the doorway in order to generate downward plane jet along the doorway. The test area was again divided into two zones. One of zones remained cold while the other was warming up during the experiment. The effect of air curtain performance while supplying the air with various velocities will be observed. This case assumes following:

- The warm air inside the warm zone rises and at the same time is distributed by the slot diffuser along the downward plane jet. Created jet reaches up the floor and enters both zones at the ground level.
- The room air from both zones is carried away by the jet and mixing in the stream.
- The plane jet force the air movement and provide better mixing of the air inside both zones.
- The warm air is supplied into the lower part of the cold and warm zone. Afterwards the warm air stream rises and mixes with the room air.
- Distributing the air downward with the plane jet may help to reduce temperature differences inside zones by forcing the warm air into bottom part of zones and additionally decrease the period of time needed to achieve the uniform thermal parameters inside the whole building.

Figure 3 presents schematic airflow distribution between warm and cold zone in case when the warm air is distributed through the slot diffuser installed above the doorway.

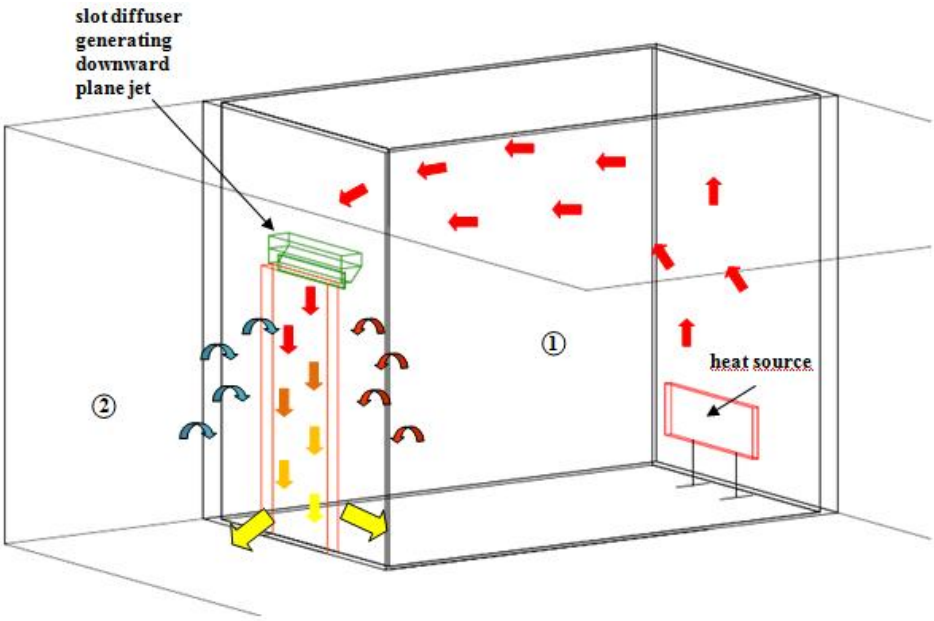

Figure 3. Schematic airflow distribution from the slot diffuser located above the opening between cold and warm zones.

3. Plane jet theory

3.1. State-of-the-art - air curtains

In general the air curtain is considered as a device producing downward plane jet which create a barrier between the two environments. Owing to a wide application of the air screens, the concept has become very popular. The air curtains are currently used to separate zones with different environment conditions, particularly to limit heat and mass transfer between this two regions. Opening door or gate between different areas can lead to significant loss of heat or cold. In order to avoid this phenomena air curtains are mounted wherever it is needed to open door or gate very often, for example: entrances to the public buildings, cooling rooms and refrigerators, as well in chemical and electronic industry. Downward plane jet can be also used to reduce the movement of toxic smoke. Therefore air curtains can be a part of fire protection system. Properly designed air curtains produce a pressure drop which forbids transversal flow through the opening. (Krajewski, 2013) However if the outlet velocity is high enough the air curtain can increase the heat and mass transfer through itself. This phenomena depends also on blowing angle.

The air curtains are also used in protect zone ventilation (PZV). Research shows that PZV systems are able to separate the room into two zones while using a slot diffuser which generate downward plane jet. Different concentration level of contaminant may be obtained on both sides of the jet. Therefore using the air curtain system as a part of PZV may protect from the cross-contaminant in a room with internal gaseous pollutant source (Cao & et al., 2011). Considering this one can assume that the air curtain system may reduce the transportation of pollutant generated from the wood stoves indoors between zones.

3.2. Theory of a free stream jet/vertical isothermal jet

The theoretical basis for air curtains analysis is a theory of a free stream jet. The free jet is formed when a fluid is discharged from outlet opening (discharge slot) (Schlichting, 1979). Excepting very small velocities of flow, it is found that the jet becomes completely turbulent at a short distance from the point of discharge. While forming the jet, discharged fluid (q_0) partly mixes with the surrounding fluid (q_{entr}) at rest. This phenomena is a consequence of the turbulence. Particles of fluid from the surroundings are carried away by the jet so that the mass-flow increases in the downstream direction. Concurrently the jet spreads out and its velocity decrease but the total momentum remains constant (Skistad, 1995); (Schlichting, 1979). *Figure 4* shows a schematic of a turbulent, plane jet.

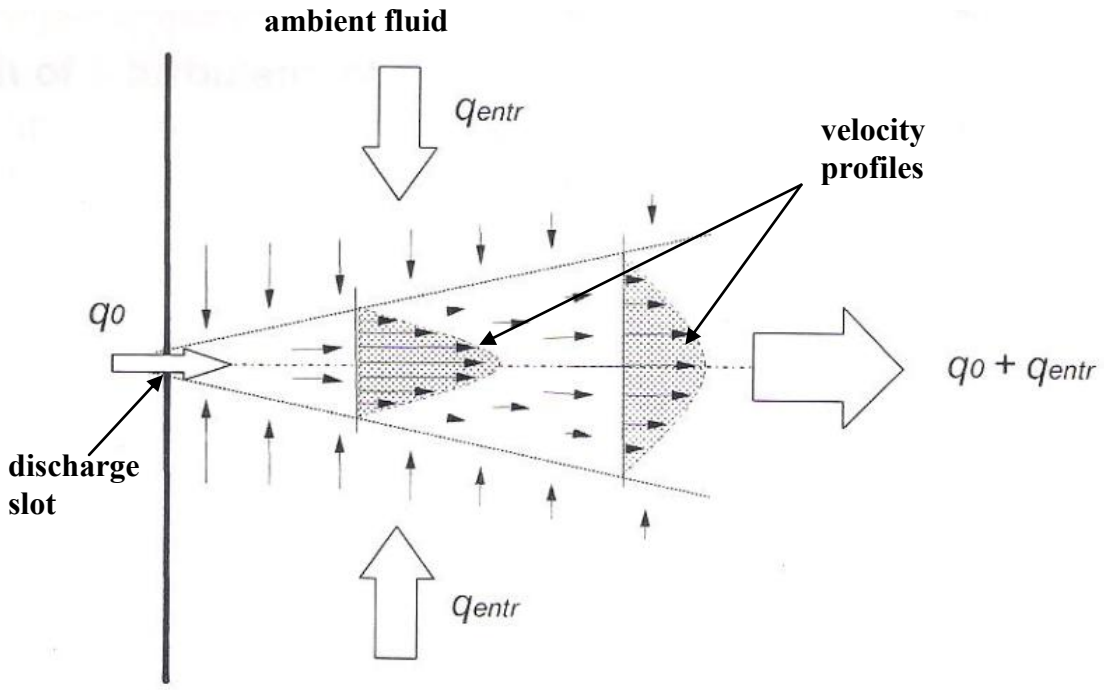

Figure 4. Air flow balance of a turbulent jet (Skistad, 1995).

3.3. Governing law: conservation of momentum

The mass and momentum fluxes are overall parameters that can be used to explore the growth of the jet in the axis of discharge slot (Essel et al. 2013). The relation of maximum

velocity along the jet u_{max} and distance from the discharge slot x can be obtained from the momentum equation.

$$\dot{j} = \dot{m} \cdot u \tag{2}$$

$$\dot{j} = \rho \cdot \dot{V} \cdot u \tag{3}$$

Where:

$\dot{j}-$ momentum flux, N, $\dot{m}-$ mass flow, kg/s, $u-$ velocity, m/s, $\dot{V}-$ volume flow, m^3/s, $\rho-$ density, kg/m^3

3.4. Velocity distribution along the jet

Considering conservation of momentum for isothermal jet studies the effect of viscosity can be neglected when modeling the maximum velocity decay. The main parameter influencing the jet behavior is the initial momentum flux M_0 from the jet slot, so the maximum velocity could be written:

$$u_{max}(x) = f_1(M_0, \rho, x)^{0.5} \tag{4}$$

Where M_0 is the initial momentum flux, ρ is the air density, x is the distance downstream of the jet slot presented (Cao, 2009).

Numerous literature positions presents subject of velocity profile and deflection of the centerline axis involving experimental data and mathematical analysis. Depending on the height and the stream of an air, the structure of the isothermal plane jet can be generally split into two regions which contains four flow zones. The first region is called the developing region and includes the potential core zone and the transition zone. The second region represents the self similarity of the jet and includes developed and impinging sectors of the jet. Particularly, depending on the height and the steam of an air, a jet shows two, three or four regions. It is possible to distinguish the potential core zone, the transition zone, and the fully developed zone or the impinging zone. Characteristic for potential core field is that the

centerline velocity is almost constant and equal to the outlet velocity u_0. The potential core takes the distance of the slot equal to 3 – 4 dimensions of a slot diameter d_N. With increasing distance from the discharge slot (until length of around seven dimensions of d_N) the stream create transition zone where the velocity decay and the jet expands. Fully developed zone is a region where velocity decay remains constant. This zone is also called main zone and occupies an area in the distance between 10 d_N and 100 d_N from the discharge slot. After that distance the jet enters impinging zone and flow becomes very complex.

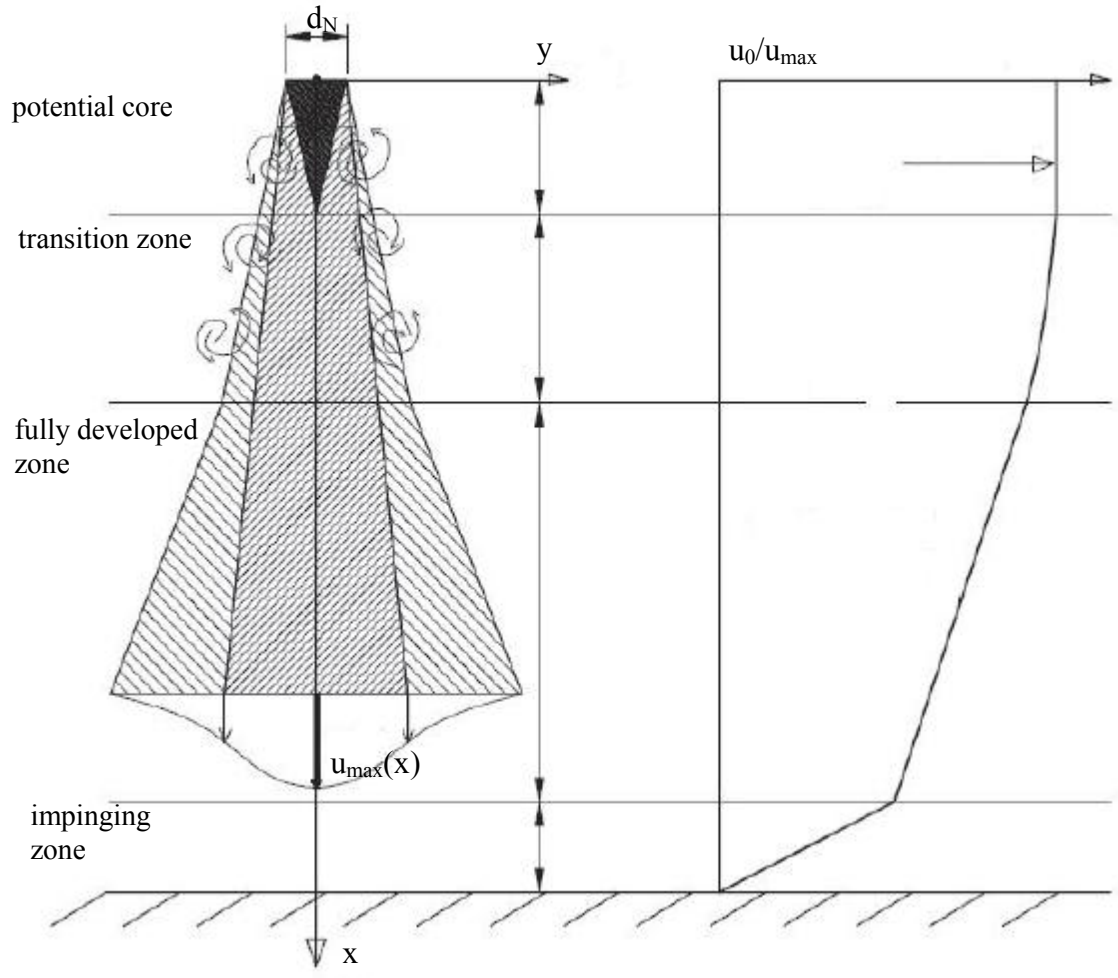

Figure 5. Schematic downward plane jet and velocity decay along the jet (Krajewski, 2013).

The centerline jet velocity in the fully developed region could be calculated from the formula based on the principle of initial momentum conservation along the jet:

$$M_0 = 2\pi\rho \int_0^{\delta} u_{max}^2 y dy \tag{5}$$

Where $M_0 = \rho u_{max}^2 A_c$ is the momentum flux M_0, where A_c is the jet slot area, δ is the distance from the axis to the jet boundary.

The velocity distribution across the jet is bell-shaped.

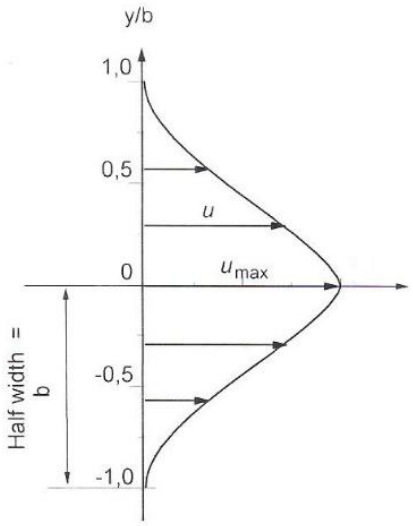

Figure 6. Velocity distribution along the jet (Skistad, 1995).

Finally the jet velocity model depends of the diffuser jet dynamic characteristic parameters and intensity of the jet velocity decay along the jet. The conventional jet model for a linear jet application can be described with formula:

$$\frac{u_{max}}{u_0} = K\sqrt{\frac{h}{x}} \tag{6}$$

Where u_{max} is the maximum air velocity, u_0 is the initial slot air velocity, K is the dynamic coefficient of the jet which depends on the slot Reynolds number if the slot Reynolds number is less than 10^4, x is the jet horizontal traveling distance, and h is the jet slot height. For the application of linear diffusers most recently K=2.67 was used for the low Reynolds number jet proposed by Skåret (Skistad, 1995).

$$\frac{u}{u_{max}} = 1 - \left(\frac{y}{b}\right)^{1,5} \quad (7)$$

Where u is velocity at the distance y from the centre line, m/s; u_{max} is velocity at the centre line of the jet, m/s.

3.5. Volume flow and width of the downward plane jet

The volume flow can be calculated accordingly to the equation:

$$q = 2l\int_0^b u\,dy = 2blu_{max}\int_0^1 \left(\frac{u}{u_{max}}\right)^2 d\left(\frac{y}{b}\right) = 2blu_{max}I_1 \quad (8)$$

where:

$$I_1 = \int_0^1 \left(\frac{u}{u_{max}}\right)\cdot d\cdot\left(\frac{y}{b}\right) = 0{,}60 \quad (9)$$

For the jet with velocity distribution of equation (6) the following expression describe momentum flux:

$$\dot{j} = 2\int_0^b u d\dot{m} = 2\int_0^b u^2\,dy = 2blu_{max}\int_0^1 \left(\frac{u}{u_{max}}\right)^2 d\left(\frac{y}{b}\right) = 2blu_{max}{}^2 I_2 \quad (10)$$

Where l is length of the air curtain, m, d is dimension of the slot, m

and:

$$I_2 = \int_0^1 \left(\frac{u}{u_{max}}\right)^2\cdot d\cdot\left(\frac{y}{b}\right) = 0{,}452 \quad (11)$$

$$\rho\cdot 2\cdot C_b\cdot x\cdot L\cdot u_{max}{}^2\cdot I_x = \dot{J} = const. \quad (12)$$

It is usually assumed that the mixing length l is proportional to the width of jet, b.

$$\frac{l}{b} = const. \quad (13)$$

In addition the rate of increase of the width, b, of the mixing zone with time is proportional to the transverse velocity.

Accordingly to (Skistad, 1995) half width of the jet can be calculated correspondingly to the expression below:

$$b = \tan\left(\frac{1}{2}\alpha\right)\cdot x = C_b\cdot x \quad (14)$$

Where:

$b -$ half width of the jet, m, $C_b -$ constant for a given angle, $\alpha -$ widening angle (20-30°),

$x -$ distance from the slot, m

The whole width of the jet refers to:

$$z = 2 \cdot b \tag{15}$$

4. Experimental setup

4.1. Measurements location

The test room was located on the second floor in the Energy and Indoor Environment Laboratory at the Department of Energy and Process Engineering at NTNU, Trondheim, Norway. The temperature in the lab, outside the climate chamber, was about 21°C. The environmental chamber was consisted of two rooms. It allows to create two zones – cold and warm. Both rooms were equipped with the same ventilation system. Ventilation system remained turned off during all laboratory work. Inside the smaller room internal heating device and air curtain system had been installed. It has been considered as the warm zone. In the further part of the report subscript 1 indicates the warm zone and subscript 2 indicate the cold zone.

4.2. Room geometry

The dimensions of the warm zone was 3.8 m length, 2.3 m width, 2.65 m height. The dimensions of the cold zone was 6.9 m length, 7.8 m width, 3.9 m height.

4.3. Internal heating device

As a heat source two different types of electric stove were used. First of them is called panel heater and second one, a convector. The devices were located differently. This was done to check the influence of the position and type of the heat source on the airflow and heat distribution within zones. The devices had different ratio of heat emitted by convection and heat emitted by radiation.

The convector can be used with both natural and forced convection by turning a fan on or off. Emission of the heat from this device is dominated by convection. For the laboratory measurements convector was running without the fan. During the experiment the convector

has been placed in two positions in order to check how location of the space heating affect the airflow distribution. The location of the heat sources can be seen in *Figure 7* and Figure 8. The heat transferred from the panel is dominated radiation. This device was equipped with the thermostat and was working in mode on/off with the maximum power consumption 800 W. Picture of panel heaters can be seen in *Attachment 2: Pictures.*

To decrease the time needed to attain steady-state all devices were set for lower power or temperature than the maximum. For all of the cases measured the heat emitters were set to the temperature of 26°C, except the convector which cannot be set to exact temperature. During the experiment the convector was not set on the maximum power. To determinate the power used by the device the intensity and voltage have been measured in the electricity plug, then the consumed/supply power was calculated and it was 1160 W.

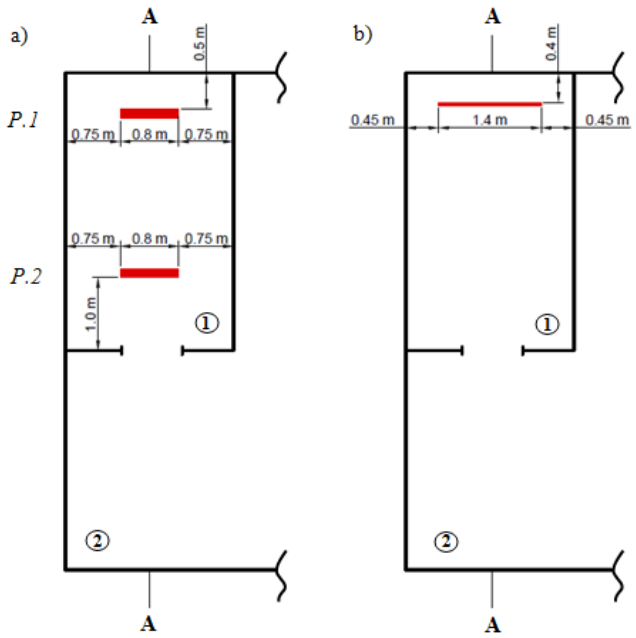

Figure 7. Location of heating devices – thrown section through the room: a) convector position *P.1* and position *P.2*; b) panel heaters

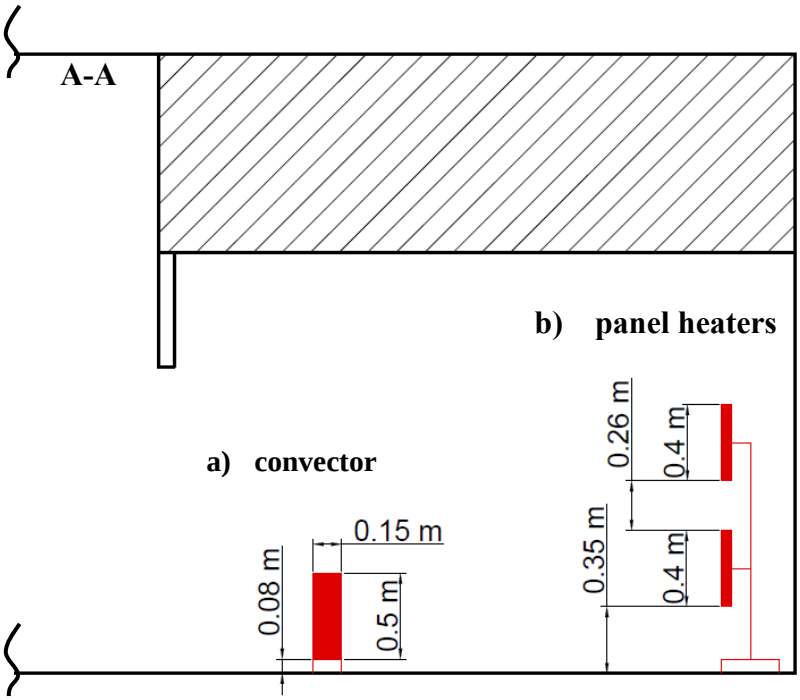

Figure 8. Dimensions of heating devices - cross section through a room a) convector; b) panel heaters

4.4. Air curtain installation

The slot, which produces downward plane jet, was install above the door inside the room. The slot has dimensions of 1 m length and 0,01 m width and was located at a height of 1,92 m above the floor. The air was sucked at the level of 2 m above the floor and was discharged from the slot to form the downward air curtain. The diameter of the pipe connecting the intake, fan and the air curtain was ø160 mm. The air curtain system can be seen in *Figure 46: Air curtain system.*

4.5. Preparation of the laboratory measurements

4.5.1. WiSensys system

WiSensys is a wireless indoor environment sensing system with data logging capability. In order to collect a major of database WiSensys sensors, platform for wireless measurements, base station WS-BU and PC software SensorGraph were used. This integrated system allows to obtain wireless signal from air temperature and velocity sensors and to present data on

graphs. The database could be exported then to an excel file. Picture of WiSensys platform can be seen in Appendix 2: Pictures.

4.5.2. Temperature measurements

In the experiment both room air temperature and surface temperature of walls were measured. To measure temperature of room air twenty WiSensys PT-100 sensors were used. Probes were mounted to telescopic, vertical poles on a certain levels in both warm and cold zone. Eight thermocouples, type T have been placed on representative points on walls inside the warm zone in order to measure the surface temperature. To gather the database from all temperature sensors compatible WiSensys devices were used.

4.5.3. Velocity measurements

To measure the velocity along the doorway ten anemometers type TSI Air Velocity Transducer 8475 were placed on the vertical pole. For this measurements predicted velocity values[1] were laying within the range of the probes which is 0 – 2.5 m/s. For all laboratory measurements and during the calibration the following settings were used:

Full scale of the velocity range	0 – 2.5 m/s
Output type	0 – 20 mA
Time constant	10 s

The transducer output is read in current signal. In order to convert signals into velocities, the following formula was used:

$$V = \frac{E_{out} - E_0}{E_{FS} - E_0} \cdot V_{FS} \tag{16}$$

V – measured velocity, m/s

V_{FS} – full scale velocity setting in m/s

E_{out} – measure output voltage or current signal

E_0 – zero flow output voltage or current

[1] Expected velocity along the doorway lies between 0 – 0.5 m/s according to theory

E_{FS} – full scale voltage or current output

The probes were connected to a sensor WiSensys WS-DLXa which allows wireless transmission of the signal to be base station. Due to the fact that device transfer the signal three times per minute the time constant were set for 10 seconds. This setting also had impact and helped to decrease fluctuations. For measurements along the plane jet of the air curtain TSI VelociCalc Plus were used. The device can measure velocities within the range from 0 m/s to 50 m/s therefore it was used for the measurements along the plane jet[2].

4.5.4. Calibration of anemometers

Calibration of velocity probes was made before start of laboratory measurements in furtherance of be sure that the probes give useable results. The calibration was carried out by using the low velocity wind tunnel. The velocity of the airflow through the tunnel is known and can be controlled by setting the air intake and the speed of the fan. For the certain speed of the fan there is proper graph which shows the relation between the opening and the airflow velocity in the tunnel. The procedure is done manually. This may cause an error while the opening is not set exactly as it should be or if the values is not read accurately enough from the line chart. All velocity probes were calibrated with the same settings:

Full scale	0.0 – 2.5 m/s
Zero	0
Span	1
Output type	0 – 20 mA
Time constant	1 s

The velocity were measured for ten set values. As provided in the instruction the accuracy of used probes is presented in the following table:

Table 1. Accuracy of Air Velocity Transducer Model 8475

Accuracy	±3.0% of reading
	±1.0% of selected full scale range
Repeatability	<±1.0% of reading

[2] Expected velocity along the plane jet lies between 0 – 10 m/s according to theoretical assumptions

The calibration outcome was that the measured values were different from the set values. Therefore, based on the accuracy, the minimum and maximum velocities have been calculated in order to check if the values lies within the margin. The results of the calibration are shown in Appendix 1: Calibration of velocity probes.

4.5.5. Summary of the measurement equipment specification

- WiSensys base station WS-BU
- WiSensys WS-DLTa-PT100

Measurement range	-100°C to +400°C
Measurement accuracy	0.1%
Measurement resolution	0.1°C

- WiSensys WS-DLTh

Measurement range	Depends on sensor type
Measurement accuracy	±0.1% ±0.5°C
Measurement resolution	0.1°C

- WiSensys WS-DLXa

Measurement range	0 – 25 mA
Measurement accuracy	±0.25% of range
Measurement resolution	25 µA

- WiSensys PT-100

Measured physical quantity	Air temperature
Accuracy	±0,1°C
Sampling frequency	1 min

- Thermocouples, type T

Measured physical quantity	Temperature surface wall
Accuracy	±0.5°C
Sampling frequency	1 min

- Air Velocity Transducer, model 8475

Measured physical quantity	Airflow velocity
Accuracy	±3.0% of reading ±1.0% of selected full scale range
Sampling frequency	1 min
Velocity range	0 – 2.5 m/s

- TSI VelociCalc Plus – Air Velocity Meter

Measurement range	0 – 50 m/s
Measurement accuracy	±3% of reading ±0.015 m/s
Measurement resolution	0.01 /s

4.6. Measurements conditions

The laboratory tests have been conducted in the environmental chamber which imitates real room with additional heating equipment, i.e. a wood stove. The power of a wood stove will change in time. It means that the peak heat output should not last very long. For this reason the time of warming up the room was set for 60 minutes for cases measured with the distribution of air generated by the air curtain. However to describe airflow distribution and heat transfer in case without using air curtain, i.e. caused only by density differences, it is crucial to achieve steady-state conditions. Therefore in these cases time of heating the zone prior to the measurements has been extended to three - four hours depending on the conditions.

4.6.1. Temperature and velocity measurements inside cold and warm zone.

The measurements of temperature were carried both inside warm and cold zone. The air temperature distribution has been measured throughout the whole height of the rooms. Two poles with the temperature probes were placed in the distance of 1.8 m from the door aperture in each zone. The sensors were located at levels: 0.15 m, 0.75 m, 1.35 m, 1.95 m, 2.55 m above the floor. On the third pole both temperature and velocity sensors were mounted. This pole was placed inside cold zone in the distance 0.9 m from doorway and has been moved manually during the measurements to three other position in the doorway. Temperature and the velocity were measured at levels: 0.13 m, 0.26 m, 0.46 m, 0.66 m, 0.86 m, 1.06 m, 1.26

m, 1.46 m, 1.66 m, 1.80 m. The picture of the pole with probes is presented in *Figure 49:* The vertical pole with the p. Thermocouples were fixed to the walls in the warm zone. The distribution of all sensors is shown on *Figure 9* and *Figure 10* below.

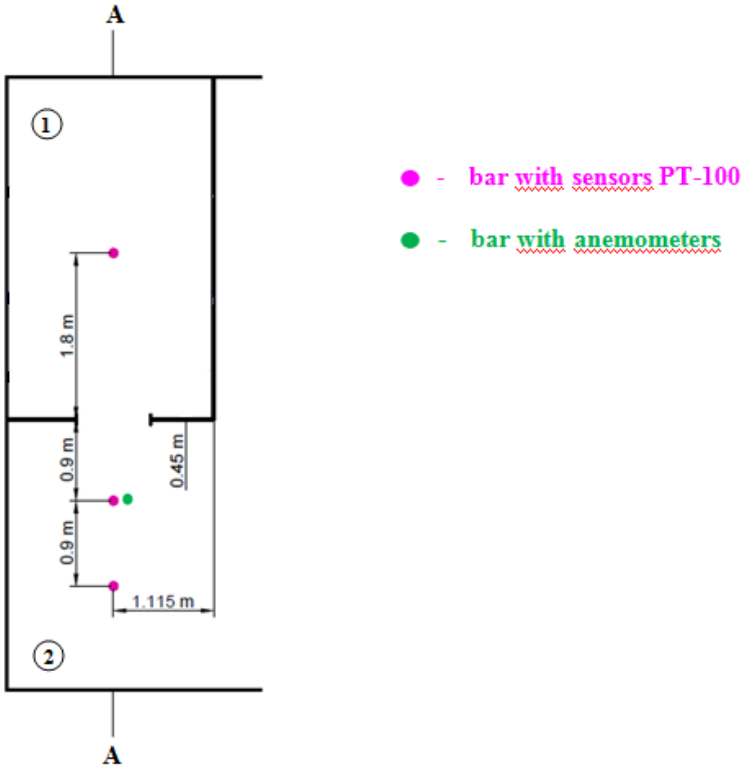

Figure 9. Location of probes, thrown section through the room.

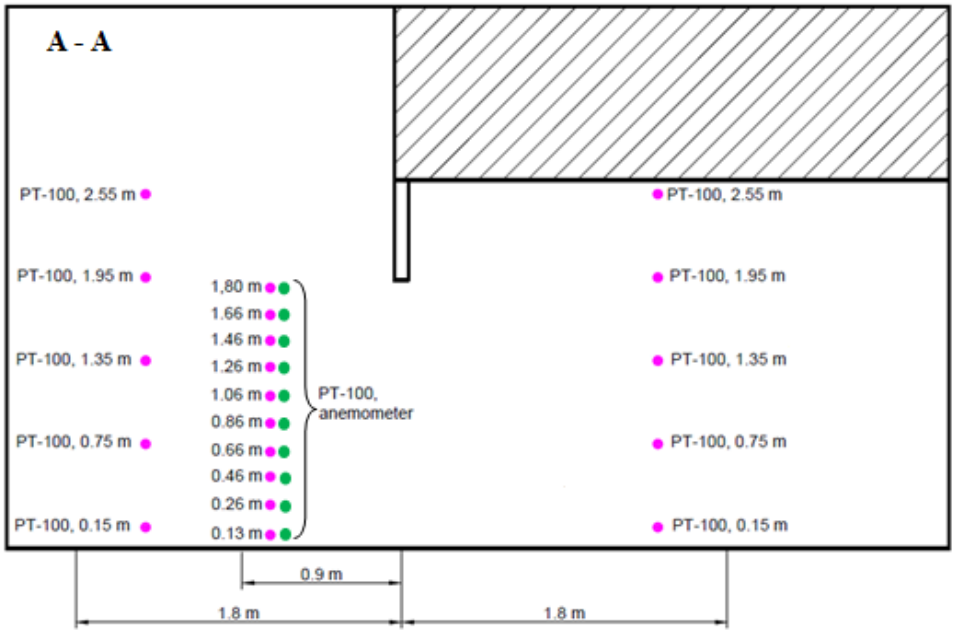

Figure 10. Location of probes, cross section through the room.

4.6.2. Laboratory measurements: without using air curtain system

The procedure starts with switching on the heating source. The initial temperature in both zones were similar. Waiting time for steady-state took around three hours. After that time appropriate measurements could be started. The values have been registered for three positions of the pole: axis of the aperture, 15 cm from right border and 15 cm from left border of the opening. Every position has been measured during the time of 10 minutes and then the average values were calculated. The pole has been moved manually and every change of the position was followed by 5 minutes break. The measurements have been done for three different cases which contains a change of space heating source and its position.

4.6.3. Laboratory measurements: using air curtain system

To describe airflow distribution while using the air curtain the same set-up have been used and the same parameters for the heat source has been set except changing the location of the heat source. The temperature inside both zones has been measured at the same locations.

Additionally the temperature distribution was measured in distance of 0.9 m from the door orifice inside cold zone. This allows to measure higher temperature values which occurs at the floor level very close to the door. The warm air is distributed downward with the jet and then it immediately mixes in a short distance inside after entering the room. It is important to check temperature distribution before the zone where the air is already mixed to identify the phenomenon of distributing warm air to the lowest part of the room.

4.6.4. Measured velocity profile along the slot and generated downward plane jet.

The measurements with the air curtain had been started with the measurement of the velocity near the slot and along the plane jet. This has been done in order to describe the jet. The flow rate from the slot were calculated based on measurements along entire width of the air curtain. The velocity was measured by TSI VelociCalc Plus within every 10 cm of the slot width. The average velocity was used to estimate the airflow volume flowing through the air curtain. The values were obtained for 3 different fan performance.

Every position and type of heat source has been measured for three different supply velocities of the plane jet: 3.8 m/s, 5.3 m/s, 8.5 m/s.

4.6.5. Summary of all conducted measurements

The summary of all conducted measurement series is presented in Tables 2,3 and 4 below:

- Series 1

Table 2. Summary of the first laboratory measurements.

Subject of measurements:	Airflow distribution along the downward plane jet
Using of air curtain system:	Yes
Discharged velocity from the slot:	
	3.8 m/s
	5.3 m/s
	8.5 m/s

Heating source:	Not used

Location of probes:	Target:
Door opening	Maximum velocity along the jet
Width of the slot diffuser	Discharged velocity profile along the slot

- Series 2

Table 3. Summary of the second laboratory measurements.

Subject of measurements:	Airflow distribution in the room
Using of air curtain system:	Yes
Discharged velocity from the slot:	
	3.8 m/s
	5.3 m/s
	8.5 m/s

Heating source type:	Position:
Panel heaters	P.1
Convector	P.1

Location of probes:	Target:	Type:	Number of probes:
Cold zone			
1.8 m from the door opening	air temperature	PT-100	5
0.9 m from the door opening	air temperature airflow velocity	PT-100 Anemometers TSI	10 10
Warm zone			
1.8 m from the door opening	air temperature	PT-100	5

- Series 3

Table 4. Summary of third laboratory measurements.

Subject of measurements:	Airflow distribution in the room
Using of air curtain system:	No

Heating source type:	Position:
Panel heaters	P.1
Convector	P.1
Convector	P.2

Location of probes:	Target:	Type:	Number of probes:
Cold zone			
1.8 m from the door opening	air temperature	PT-100	5
Warm zone			
1.8 m from the door opening	air temperature	PT-100	5
Axis of the doorway	air temperature airflow velocity	PT-100 Anemometers TSI	10 10
15 cm from left border	air temperature airflow velocity	PT-100 Anemometers TSI	10 10
15 cm from right border	air temperature airflow velocity	PT-100 Anemometers TSI	10 10

4.6.6. Visualization of the air flow

Smoke visualization tests were made in order to identify the airflow patern and to determine the optima sensor locations. Due to the fact that it is hard to predict the airflow distribution, smoke visualization is then highly meaningful. In order to visualize the flow pattern of the plane jet the smoke test was prepared. The room air with smoke was supplied to the air curtain system and discharged from the slot with the downward jet. The smoke generator was also used to visualize bidirectional airflow thought the doorway. In this case the warm zone needed to be warm up and steady-state regime had to be reached. If these conditions are attained the smoke can be supplied directly to the zone at the bottom level.

5. Results

The conditions of the laboratory measurements differ between the baseline case and measurements with the air curtain system and the results will therefore be discussed and compared after each part of the chapter.

5.1. Series 1: Measurements of downward plane jet.

Turbulent transport phenomena and mixing characteristics of turbulent jets are specifically influenced by the configuration of a slot diffuser. In order to widen the knowledge about the effect of slot diffuser performance the following measurements have been conducted: visualization of the downward plane jet with using the smoke, measurements of velocity profile along the slot and measurements of velocity along the downward plane jet. More detailed description of he conducted measurements can be found below.

5.1.1. Visualization of the downward plane jet without heater in the room.

The smoke test was conducted for three different supply velocities from the slot: 3.8 m/s, 5.3 m/s and 8.5 m/s. Those velocities were also set for all experiment cases with using air curtain system. The pictures were taken from the side of the cold zone so the distribution of the air was visible only on that side. The doorway can be seen on the right side of the pictures. The slot diffuser can be seen in the upper right corner. The pole on the pictures represents the distance of 1.8 m from the downward plane jet. The red arrows indicate the direction of airflow as was observed while conducting the experiment with the smoke. While conducting the test with smoke the ambient conditions could vary slightly between the cases. The results of the test are presented in the pictures below.

- Discharged velocity from the slot equal to 3.8 m/s

Figure 11 shows formation of the downward plane jet. The picture was taken after 10 s from starting supply the smoke through the air curtain system. Only half of the jet can be seen, while the half of the jet remains invisible on side of the warm zone. The jet starts to spread out in a short distance from the slot. The red arrows show the direction of the flow.

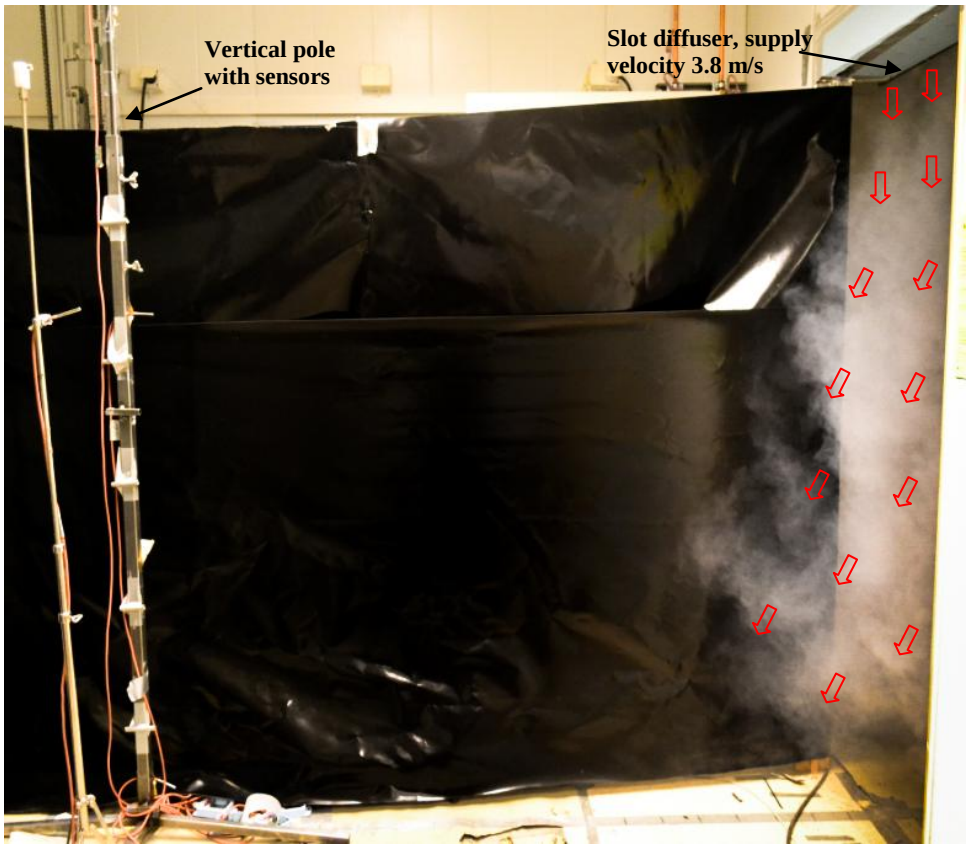

Figure 11. Downward plane jet distributed inside cold zone, discharged velocity 3.8 m/s, t=10 s.

Figure 12 and *Figure 13* show the airflow distribution after time of 20 s and 30 s. It can be seen on the *Figure 12* that while the jet reached the floor the air changed direction of flowing. The air moves along the floor inside the room. Before reaching the distance of 1,8 m, jet visualized by smoke changes direction again and moves upward the room. The blue arrows illustrates the cold air which is carried away into stream. In the neighborhood of these arrows slight wires can be seen. After about 30 s. the air with smoke mixes with the room air which can be seen in *Figure 13*. The red arrows show the direction of the flow.

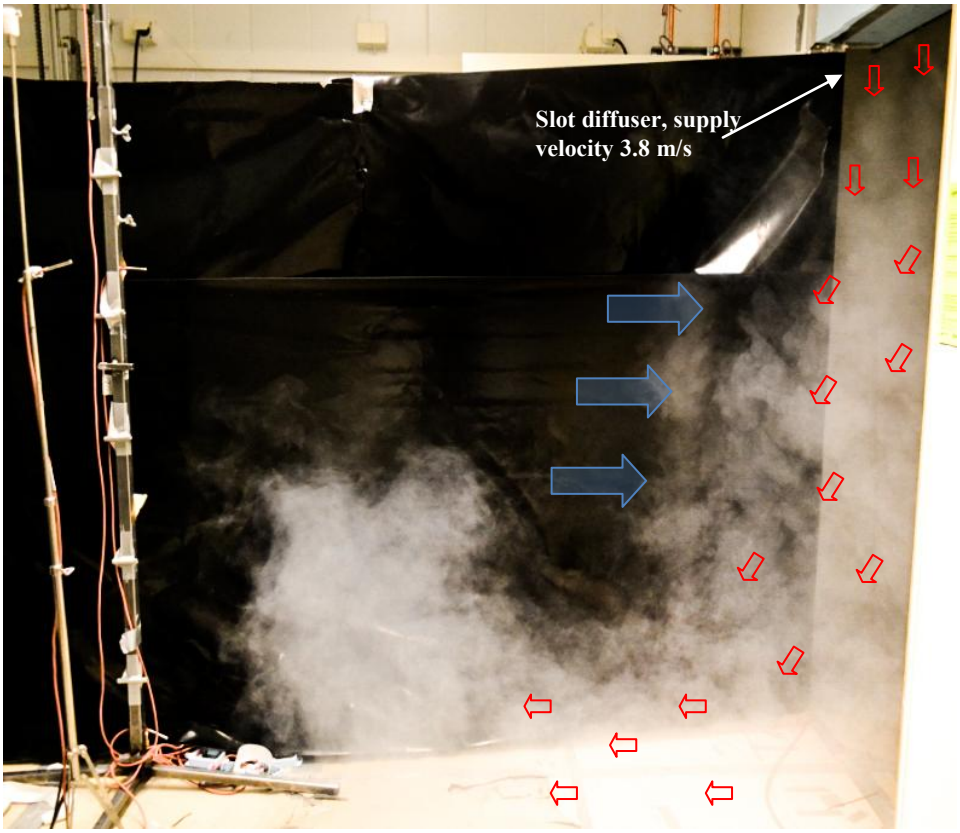

Figure 12. **Airflow distribution inside cold zone, discharged velocity 3.8 m/s, t=20 s.**

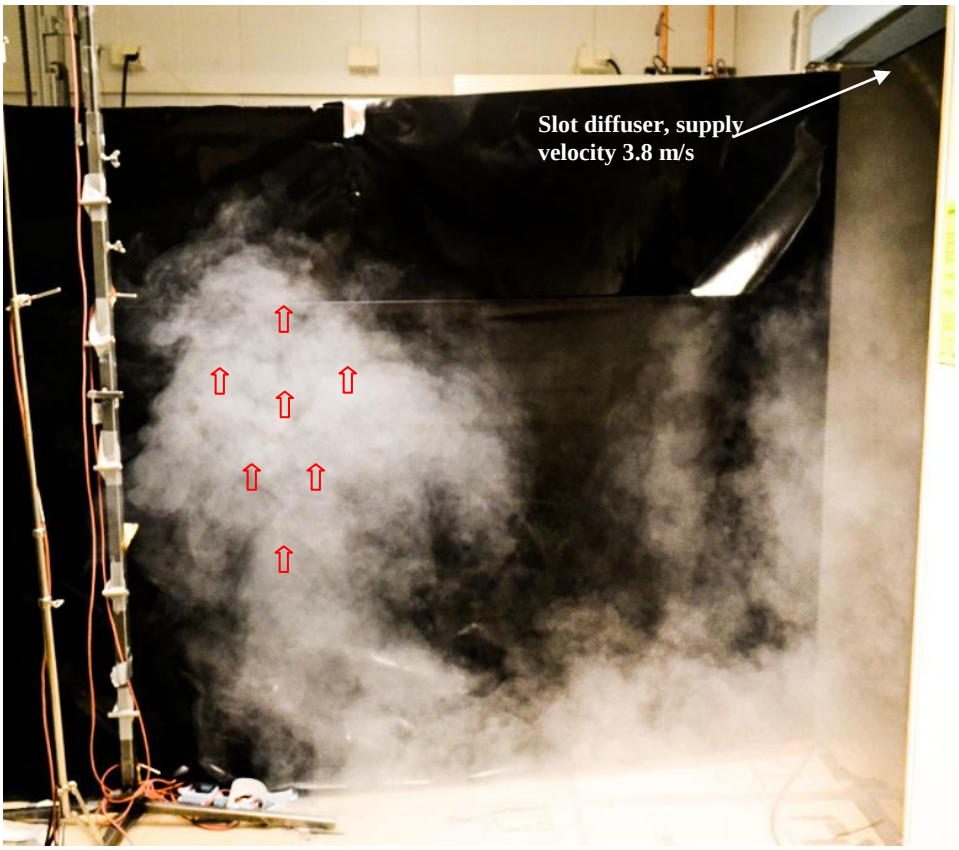

Figure 13. **Airflow distribution inside cold zone, discharged velocity 3.8 m/s, t=30 s.**

- Discharged velocity from the slot equal to 5.3 m/s

Figure 14, *Figure 15* and *Figure 16* present the flow pattern for velocity supplied from the slot equal to 5.3 m/s. The performance is analogous to the previous conduct and pictures were taken after 10, 20 and 30 s after starting supply the smoke.. The air was discharged from the slot diffuser located above the door opening and directed downward. The blue arrows on *Figure 14* illustrates the cold air which is carried away into stream. On *Figure 15* the air distributed with the jet enters the room. The smoke also occupies higher levels in the short distance from the door opening similar as it is presented on *Figure 112*. *Figure 16* shows the air distribution after around 30 s. It can be seen that the smoke evenly fills the room. The air with smoke mixes with room air and goes upward. It occupies the space between the door aperture and the pole with sensors.

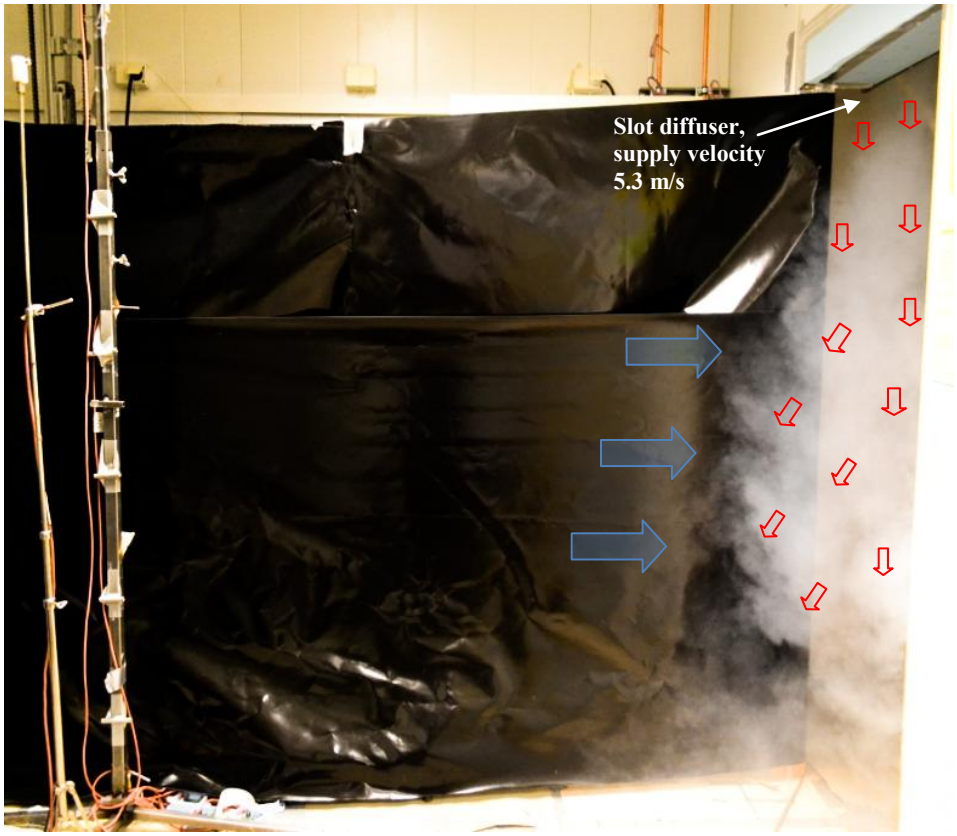

***Figure 14*. Downward plane jet distributed inside cold zone, discharged velocity 5.3 m/s, t=10 s.**

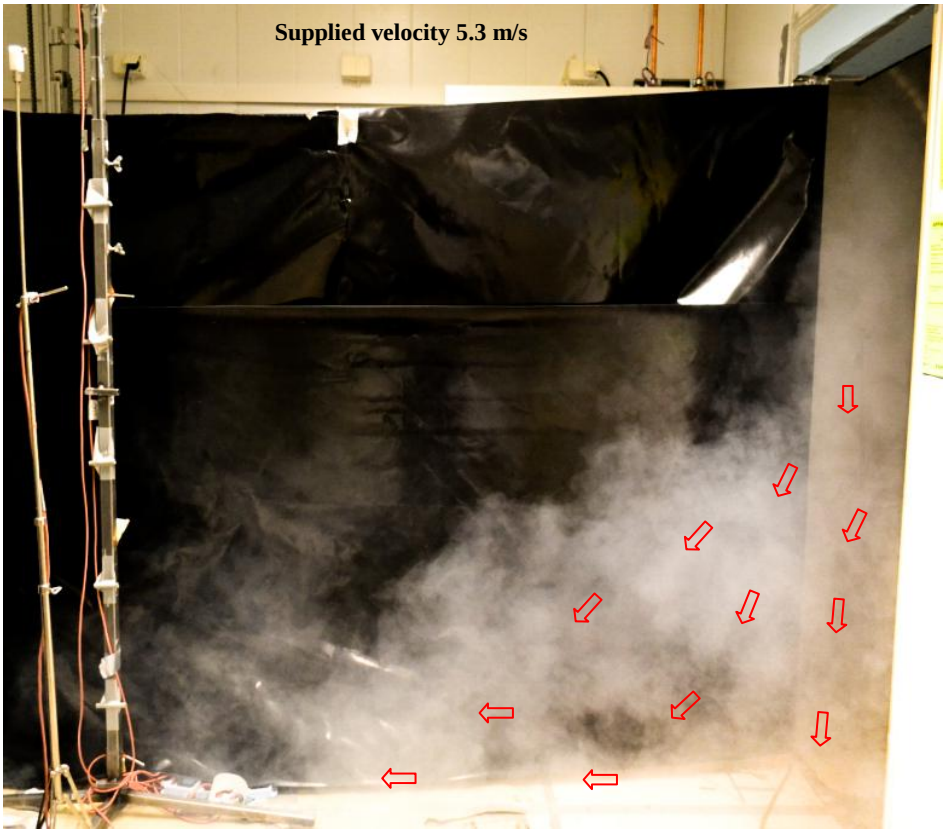

Figure 15. **Airflow distribution inside cold zone, discharged velocity 5.3 m/s, t=20 s.**

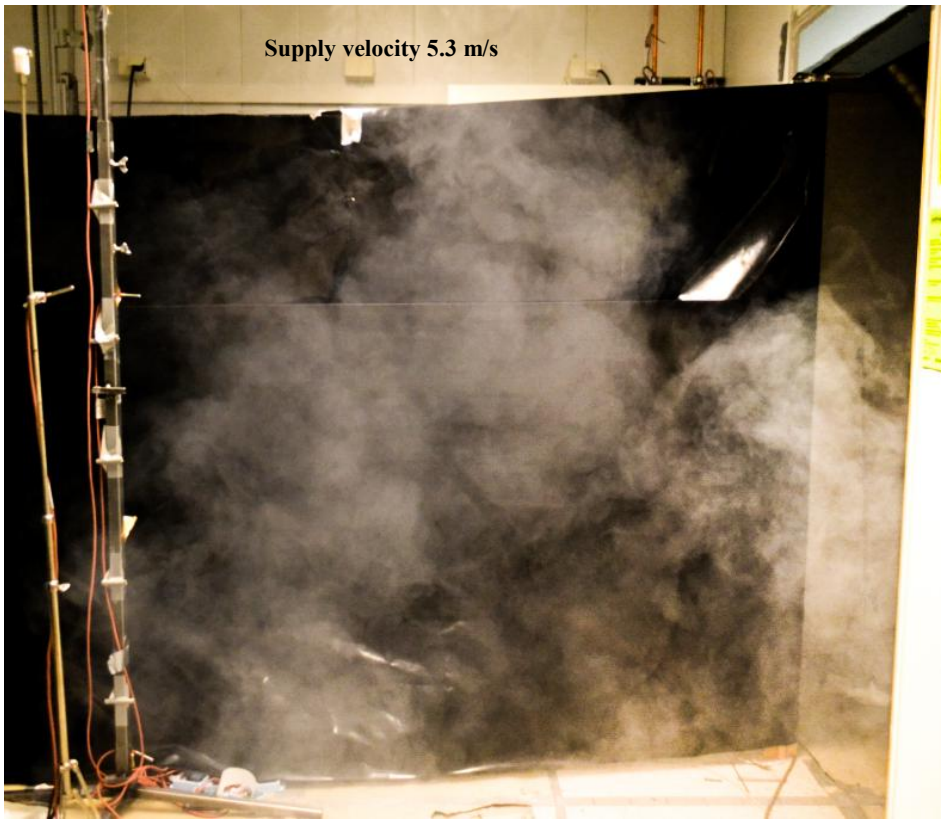

Figure 16. **Airflow distribution inside cold zone, discharged velocity 5.3 m/s t=30 s.**

- Discharged velocity from the slot equal to 8.5 m/s

Figure 17, *Figure 18* and *Figure 19* visualize the airflow distribution while the discharged velocity was equal to 8.5 m/s. The high smoke concentration can be seen on *Figure 17* in a right bottom region near the door. The plane jet along the doorway is thinner than for lower supplied velocities (*Figure 11* and *Figure 14*). When the plane jet reached the floor, the airflow changed direction. The air is pushed into room and moves horizontally towards the vertical pole. At the same time the smoke mixes with the room air (*Figure 17*, *Figure 18*). The stream floats up after crossing the further distance from the door, on the right of the pole. This can be seen on left side of *Figure 18* and *Figure 19* in the neighborhood of the pole with sensors.

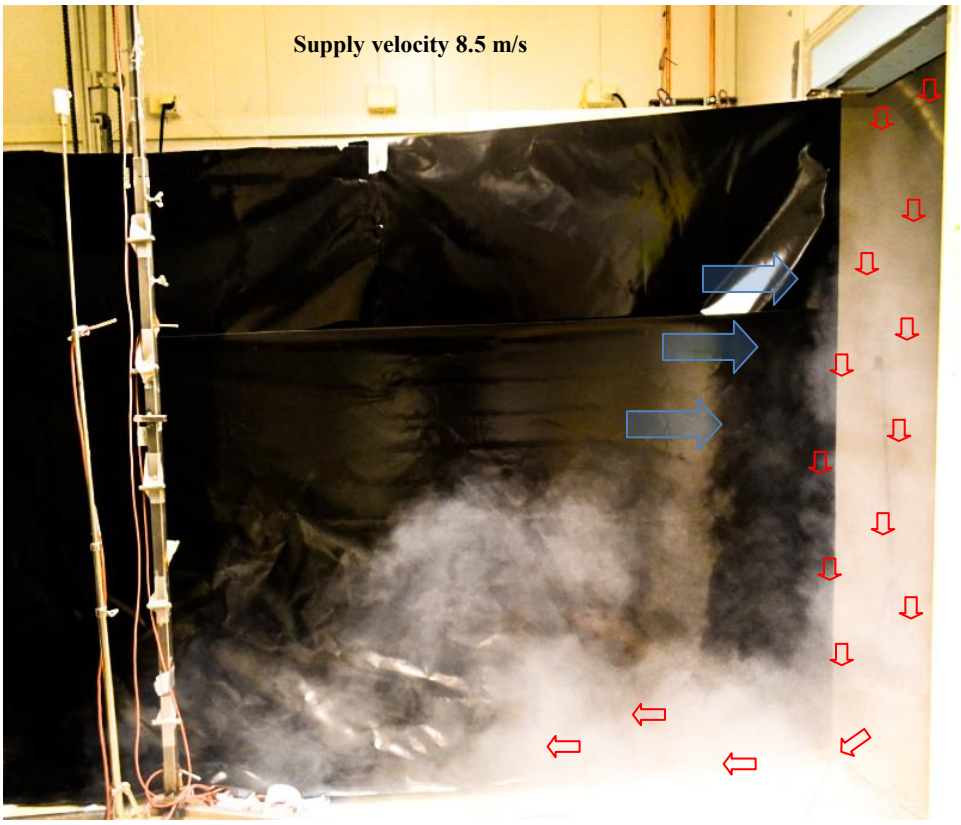

Figure 17. **Downward plane jet distributed inside cold zone, discharged velocity 8.5 m/s, t=10 s.**

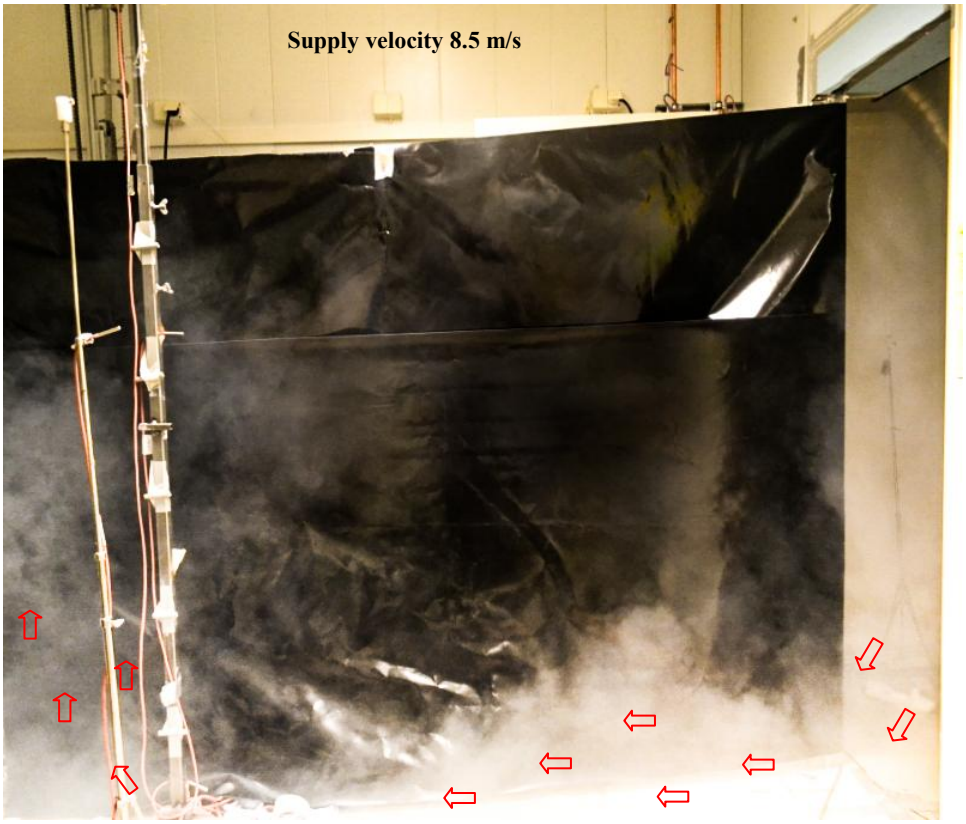

Figure 18. **Airflow distribution inside cold zone, discharged velocity 8.5 m/s t=20 s.**

Figure 19. **Airflow distribution inside cold zone, discharged velocity 8.5 m/s, t=30 s.**

The outcomes of the visualization are following: the warm air was distributed downward from the slot and reached down the floor. Afterwards the warm air was going up immediately and started to mix with the air inside cold zone. For lower velocity the warm air started to rise in shorter distance from the doorway than for higher velocity. For discharged velocity equal 3.8 m/s this distance was less than 1.8 m. For discharged velocity equal 8.5 m/s the warm air was distributed at bottom level and started to go up after crossing the distance of 1,8 m. For velocity 5.3 m/s the air started to go up exact at distance of 1.8 m.

In a short time (30 s.) distributed air mixed with the cold air and the smoke was distributed evenly inside cold zone.

5.1.2. Measurements of velocity profile along the slot

The velocity were measured directly near the slot of the diffuser. The values were measured according to the description presented in Chapter 4.6.4 The average velocity was used to estimate the airflow volume flowing through the air curtain. The values were measured for 3 different fan performance. The results are present in Table 5. Discharge velocity from the slot of the diffuser.

Table 5. Discharge velocity from the slot of the diffuser.

Fan performance	*Width of the slot, cm*									*Average velocity, m/s*
	10	*20*	*30*	*40*	*50*	*60*	*70*	*80*	*90*	
	Velocity, m/s									
(1)	3.65	3.58	3.63	3.70	3.80	3.78	3.71	3.85	4.25	**3.77**
(2)	6.40	5.05	4.72	4.64	4.60	4.90	4.89	6.55	6.30	**5.34**
(3)	9.15	8.40	8.60	8.50	8.25	8.40	8.25	7.40	9.10	**8.45**

Figure 1 shows the discharged velocity profile along the slot. It can be seen on a profile that for first fan performance the velocity was distributed almost evenly along the whole width of

the slot. For second and third fan performance discharged velocity values between 20th cm and 70th cm of the slot were similar. On both ends of the slot higher velocity was reported.

For all supplied velocities measured velocity profiles in the middle part of the slot were aligned. Therefore further measurements of downward plane jet were conducted in the middle of the width of the slot.

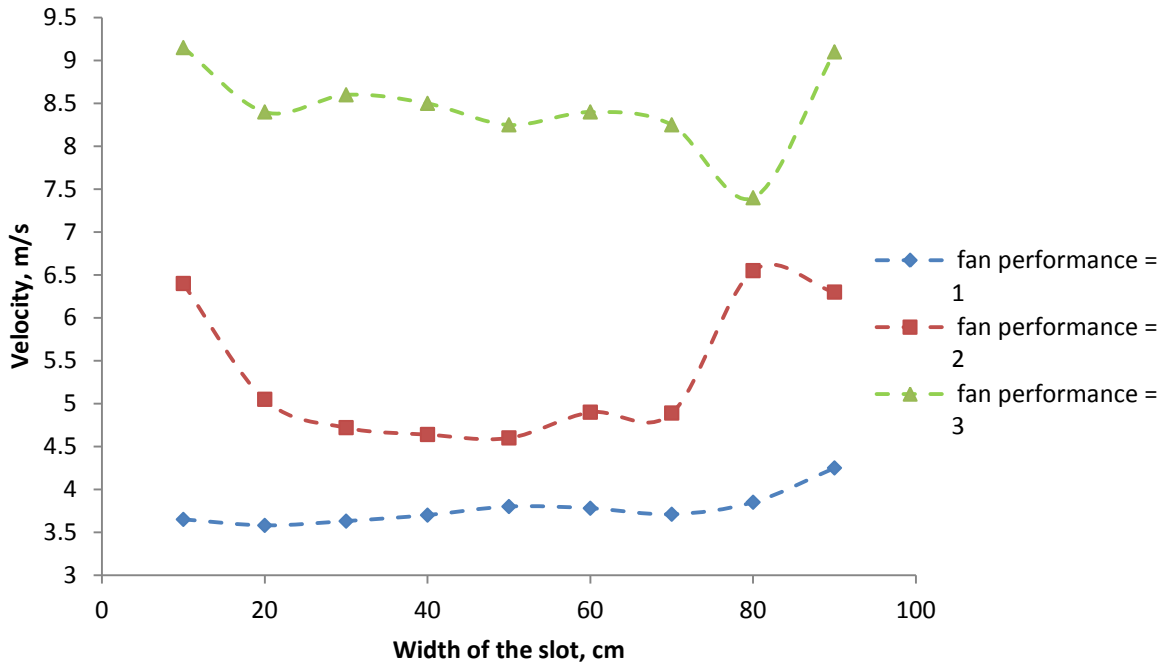

Figure 20. **Discharged velocity from the diffuser**

In order to estimate the supplied airflow volume, it has been calculated from the average velocity and the area of the slot according to the equation (17).

$$Q_{sl,i} = A_{sl} \cdot u_{av} \tag{17}$$

$Q_{sl,i}$ – Volume of the supplied air, m^3/s

A_{sl} – Area of the slot, m^2

u_{av} – Average velocity, m/s

The flow rate calculation shows Table 6.

Table 6. Calculation of the supplied air volume.

Fan performance	*Average velocity, m/s*	*Area of the slot, m^2*	*Volume of the supplied air, m^3/s*	*Volume of the supplied air, m^3/h*
(1)	3.77	0.01	0.038	**135.8**
(2)	5.34	0.01	0.053	**192.2**
(3)	8.45	0.01	0.085	**304.2**

5.1.3. Measurements of velocity along downward plane jet

The maximum velocity along the plane jet has been measured. Based on the obtained values coefficient *k* was calculated according to the formula (19):

$$\frac{u_{max}}{u_0} = k \cdot \sqrt{\frac{h}{x}} \tag{18}$$

$$k = \frac{u_{max}}{u_0} \cdot \frac{1}{\sqrt{\frac{h}{x}}} \tag{19}$$

h – width of the slot, 0,01 m

x – distance from the slot, m

Table 7 present outcomes from measurements of maximum velocity along the jet and calculated coefficient *k*.

Table 7. Measured u_{max} values along the jet and calculated coefficient k values.

	Supply velocity					
	3.8 m/s		**5.3 m/s**		**8.5 m/s**	
Distance from the slot, m	*u_{max}, m/s*	*Coefficient k*	*u_{max}, m/s*	*Coefficient k*	*u_{max}, m/s*	*Coefficient k*
0.2	1.80	**2.12**	2.65	**2.24**	4.40	**2.31**
0.4	1.60	**2.66**	2.29	**2.73**	3.50	**2.60**
0.6	1.32	**2.69**	1.85	**2.70**	2.66	**2.42**
0.8	1.17	**2.75**	1.43	**2.41**	2.40	**2.53**
1.0	0.87	**2.29**	1.22	**2.30**	1.90	**2.24**
1.2	0.81	**2.34**	1.03	**2.13**	1.70	**2.19**
1.4	0.64	**1.99**	0.97	**2.17**	1.50	**2.09**

Figure 21 presents the maximum velocity decay along the plane jet as a function of streamwise distance. For all cases the biggest velocity decay can be observed in the distance from 0 m to 0.2 m from the discharging point. In the middle of the jet, at the length of 0.4 m, 0.6 m, 0.8 m and 1 m the velocity decrease was still considerable. After the distance of 1 m the velocity differences were much smaller and the velocity profile became more flat.

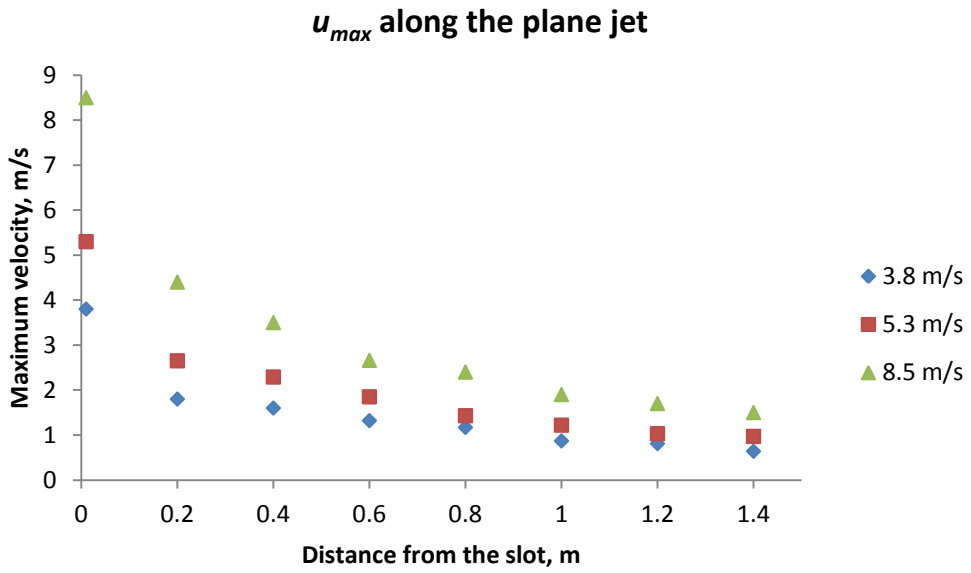

Figure 21. **Maximum velocity along the plane jet for supply velocities: 3.8 m/s, 5.3 m/s and 8.5 m/s.**

The coefficient *k* is specific for the geometry of the device which generate downward plane jet. According to the literature (Skistad, 1995) the value of coefficient *k* should lie between 2.60 – 2.70. The velocity profile along the jet was then compared with the theoretical values of the u_{max} calculated accordingly to equation (21):

$$\frac{u_{max}}{u_0} = 2.67 \cdot \sqrt{\frac{h}{x}} \tag{20}$$

$$u_{max} = 2.67 \cdot \sqrt{\frac{h}{x}} \cdot u_0 \tag{21}$$

Figure 22, *Figure 23* and *Figure 24* display the measured and calculated maximum jet velocity in the centre line of the plane jet.

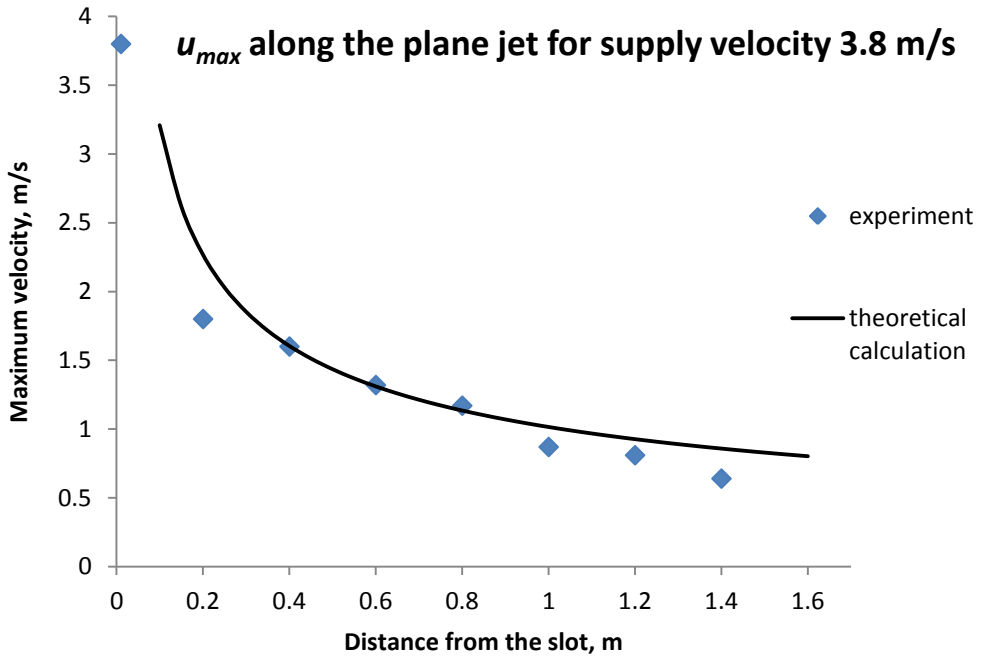

Figure 22. Measured and calculated maximum velocity along the plane jet, supply velocity 3.8 m/s

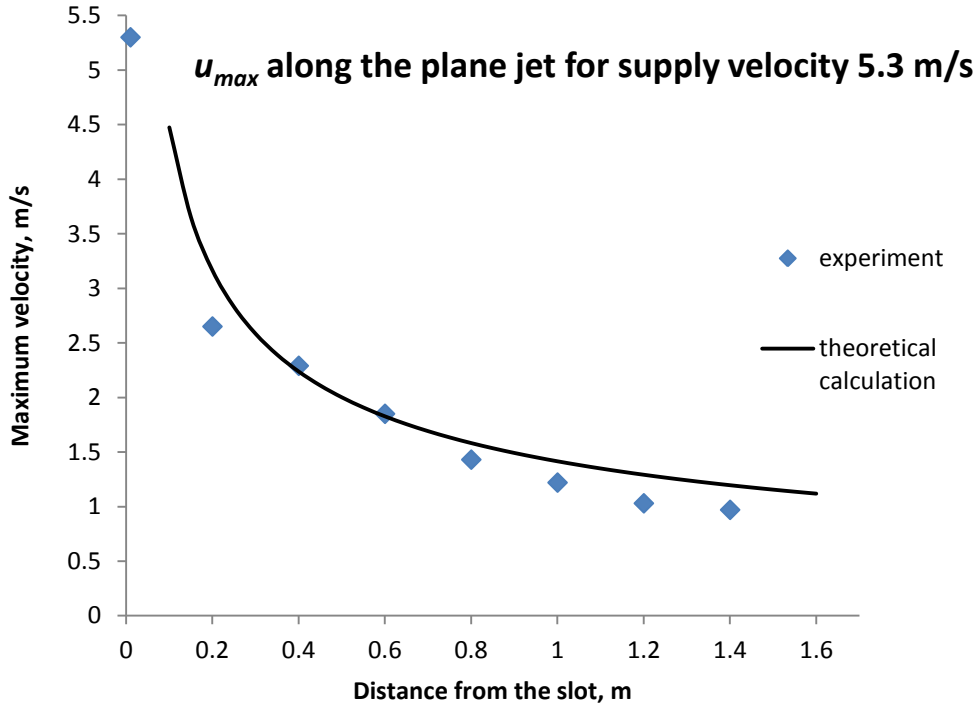

Figure 23. Measured and calculated maximum velocity along the plane jet, supply velocity 5.3 m/s

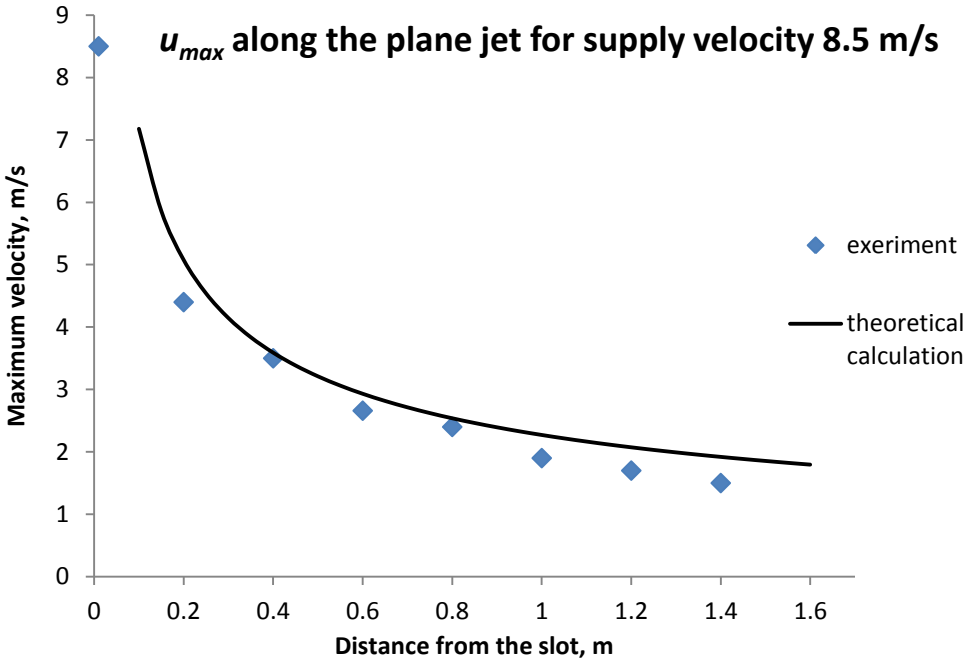

Figure 24. **Measured and calculated maximum velocity along the plane jet, supply velocity 8.5 m/s**

The results showed that discharged velocity influence the performance of an air curtain. For all cases measured values were similar to calculated values where the distance from the slot was equal to 0.4 m and 0.6 m. The biggest differences were recorded in the distance of 0.2 m. In general the shape of the velocities profiles were comparable. These results indicate that the calculated results fit closely to the measured data with only marginal errors.

5.1.4. Conclusions

The experimental investigation was undertaken to study the characteristic of downward plane jet generated by slot diffuser located above the door opening. The decay of the centerline mean velocity were obtained to evaluate the mixing characteristic. The smoke test was conducted to visualize the airflow distribution both along the plane jet and inside the cold zone. The results demonstrated following:

- The air supplied from the slot diffuser create downward plane jet which cover the whole width of the door opening and reach down to the floor. The jet volume increase

with increasing the distance from the discharging point. At floor level the jet change direction and the distributed air is entering both zones. The distance it enters inside the room depends on discharged velocity created jet. In a short time the jet air mixes with surrounding air.

- Considering the discharged velocity profile, it can be seen that the air is supplied evenly in the middle part of the slot but on the endings the velocity is slightly higher. This trend is more visible for higher velocity values.
- Due to the inward entrainment of the ambient air into the jet, the streamwise mean velocity values decay and volume spread out progressively with increasing distance from the slot.
- Decay of centerline mean velocity of the jet, for the slot diffuser investigated in this study complies with the results obtained from calculation.

5.2. Series 2: Measurements of airflow distribution with air curtain system.

This part of the chapter analyzes airflow distribution inside two rooms – cold and warm zone, while the downward plane jet was generating by air curtain system. In this part of measurements the heat source was placed in the warm zone and remained turned on during all experimental tests. Two different cases with different types of the heat source were evaluated . The indoor environment conditions and discharged velocity from the slot diffuser remained the same for both scenarios.

5.2.1. Case 1: Two panel heaters used as the heat source in position *P.1*

The part below presents results of measured air temperature and velocity in case when the warm zone was warmed up by two panel heaters and the air curtain system remained turned on. Discharged velocity from the slot diffuser was increased during the measurements by changing the fan performance.

5.2.1.1. Temperature distribution

Results of temperature measurements in the distance of 0.9 m from the door aperture inside cold zone are presented in Table 8. The temperature values are averaged over a ten minutes measurement.

Table 8. Temperature distribution inside cold zone in the distance of 0.9 m from the downward plane jet.

	Supply velocity		
	3.8 m/s	**5.3 m/s**	**8,5 m/s**
Height, m	*Temperature, °C*		
1.8	23.1	22.3	20.9
1.66	23.2	22.2	20.8
1.46	23.3	22.1	20.9
1.26	23.4	21.9	21.0
1.06	23.2	21.7	21.2
0.86	22.6	21.4	21.3
0.66	22.0	21.2	21.7
0.46	21.3	21.4	22.0
0.26	20.7	21.1	22.3
0.13	20.7	21.1	22.7

There were small differences between initial temperature inside both zones each time when starting the heating during the experiment. Therefore the temperature values between cases cannot be compared directly, only distribution or gradient can be analyzed.

Temperature distribution inside cold zone in the distance of 1.8 m from the downward plane jet is presented in Table 1Table 9.

Table 9. Temperature distribution inside cold zone in the distance of 1.8 m from the downward plane jet.

	Supply velocity		
	3.8 m/s	**5.3 m/s**	**8,5 m/s**
Height, m	*Temperature, °C*		
2.55	22.3	22.1	20.8
1.95	21.9	21.6	20.6
1.35	21.3	21.3	20.3
0.75	20.8	21.0	20.1
0.15	20.5	20.9	19.8

Based on the results presented in **Błąd! Nie można odnaleźć źródła odwołania.**Table 8 the following observation were made: at the point distant 0.9 m from the downward plane jet and for the lowest supply velocity, in this case equal to 3.8 m/s, the lowest temperature value was registered by two sensors located at levels 0.15 m and 0.26 m. Then temperature increased with the altitude. The highest temperature value was recorded at the level of 1.26 m. At upper levels the temperature decreased insignificantly from 23.4 °C to 23.1 °C. Inverted situation can be seen in case with supply velocity equal to 8.5 m/s. In this case the highest temperature value was obtained at the level of 0.15 m. The temperature decreased significantly with altitude and then at the level of 1.8 m increased slightly. The smallest difference between temperature values measured at the lowest and the highest level was recorded for the supply velocity 5.3 m/s. In this case temperature increased with the height. The probe located at height 0.46 m was a bit warmer than the upper probes. The temperature distribution distant 0.9 m from the jet is presented in Figure 25.

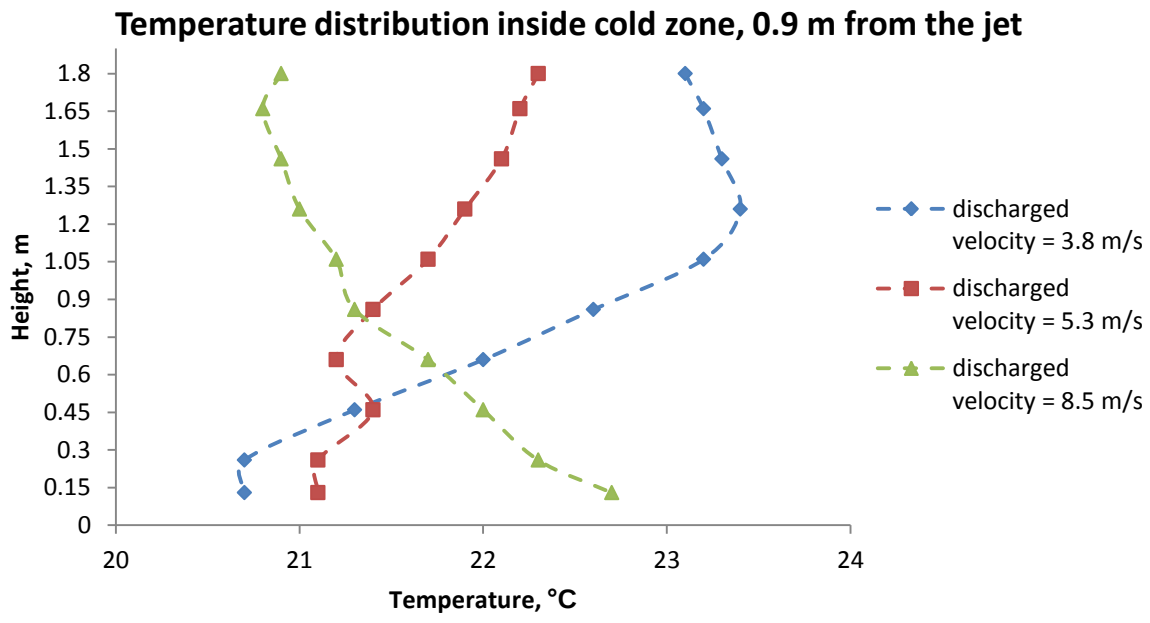

Figure 25: Temperature distribution inside cold zone in the distance of 0.9 m from the plane jet. Blue color refers to discharging velocity from the slot 3.8 m/s, red color refers to velocity 5.3 m/s, green color represent velocity of 8.5 m/s

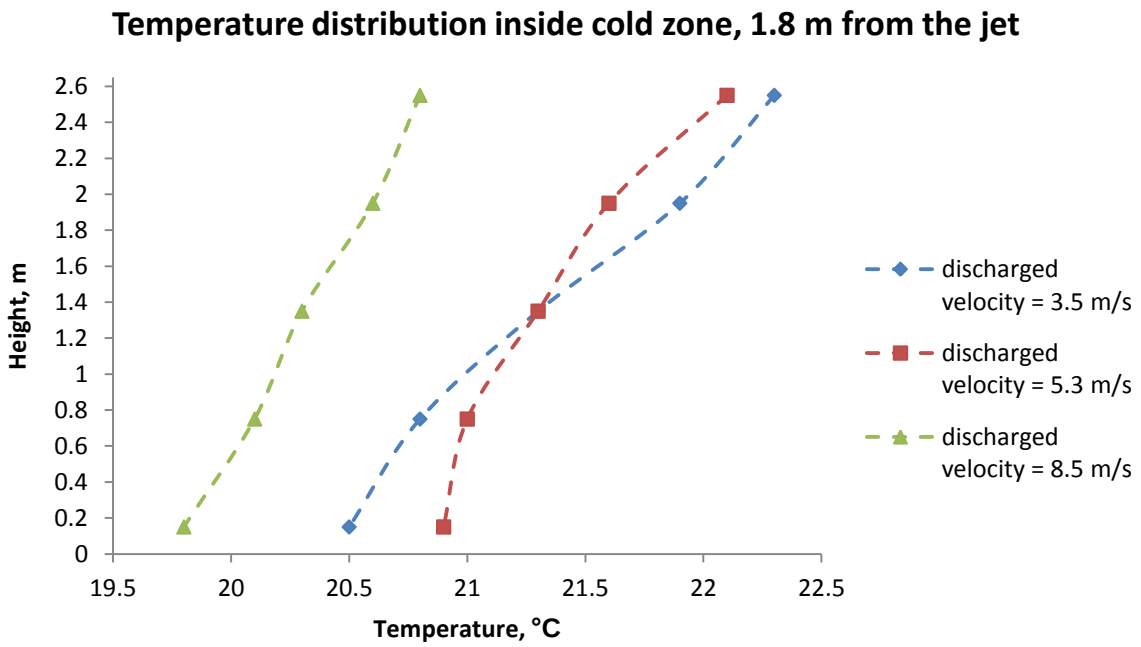

Figure 26: **Temperature distribution inside cold zone in the distance of 1.8 m from the plane jet. Blue color refers to discharging velocity from the slot 3.8 m/s, red color refers to velocity 5.3 m/s, green color represent velocity of 8.5 m/s**

Figure 26 presents temperature distribution in bigger distance – 1.8 m from the jet. At this point temperature increased with altitude for all supply air velocities. However it can be seen that temperature difference between the lowest and the highest located probes decreased with increasing velocity. For supply velocity 3.8 m/s the temperature difference between level of 0.15 m and 2.55 m was 1.8 °C while for supply velocities 5.3 m/s and 8.5 m/s the difference was 1.2 °C and 1 °C. Comparison of Figure 25 and Figure 26 indicates that with increasing discharged velocity the warm air passes longer distance before starting to mix and going upward.

The temperature distribution inside warm zone is presented in *Table 10* and *Figure 27*. In case with discharged velocity 3.8 m/s the distinction between heated and unheated air was clear. The temperature distribution at the distance 1.8 m from the doorway was similar to air distribution with natural convection. The biggest temperature difference occurred between 1.35 m and 1.95 m. The change of the trend line at this level was observed also for other

supplied velocities. While increasing the velocity supplied from the slot the temperature stratification decreased significantly.

Table 10. Temperature inside warm room at the distance of 1.8 m from the jet.

	Supply velocity		
	3.8 m/s	**5.3 m/s**	**8,5 m/s**
Height, m	*Temperature, °C*		
2.55	28.2	27.7	26.4
1.95	27.0	26.8	25.6
1.35	24.7	25.9	25.2
0.75	24.0	25.5	24.9
0.15	22.9	25.1	24.6

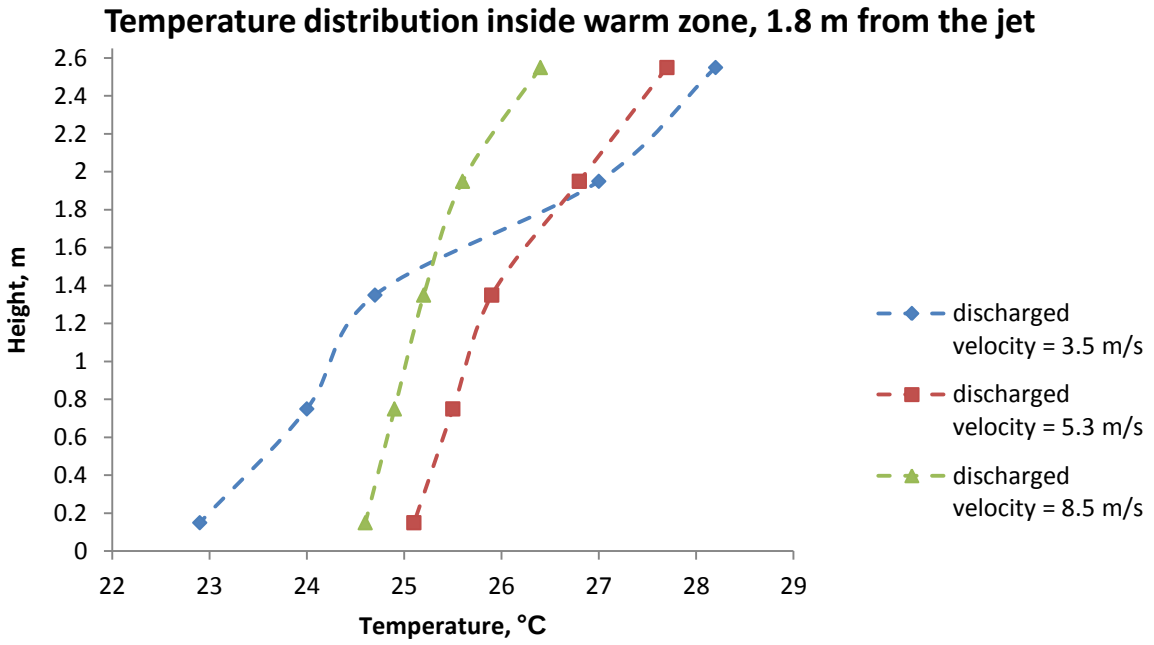

Figure 27: **Temperature distribution inside warm zone in the distance of 1.8 m from the plane jet. Blue color refers to discharging velocity from the slot 3.8 m/s, red color refers to velocity 5.3 m/s, green color represent velocity of 8.5 m/s**

5.2.1.1. Velocity distribution

Velocity distribution inside cold zone is presented in *Figure 28*. It can be seen that for supplied velocity 3.8 m/s and 5.3 m/s the graph shows similar trend while in case where supplied velocity is 8.5 m/s the trend is opposite than for the lower supplied velocities.. In cases when discharged velocity was 3.8 m/s and 5.3 m/s upper velocity probes measured the

highest values. Three probes, located at 1.8 m, 1.66 m and 1.46 m above the floor indicated similar values. Then slightly velocity growth can be seen between level of 1.06 m and 1.26 m from the floor. Below the level 0.46 m the velocity decreased. In this region the largest differences between measured values can be also observed. While supplying the air with velocity equal to 3.8 m/s three lowest probes measured almost the same temperature. For supplying velocity 5.3 m/s the values measured at the same level showed a little increase.

Green line in *Figure 28* represent measurements results for the highest supply velocity of 8.5 m/s. It can be seen that the line has different trend then the line for lower supplied velocities. In this case the highest values were measured near the floor level: 0.13 m and 0.26 m above the floor. These values are similar to the values measured by upper probes in cases with lower discharged velocity from the slot diffuser. Then the velocity decreased with altitude along the whole measured height. The highest probe measured velocity equal to 0.07 m/s.

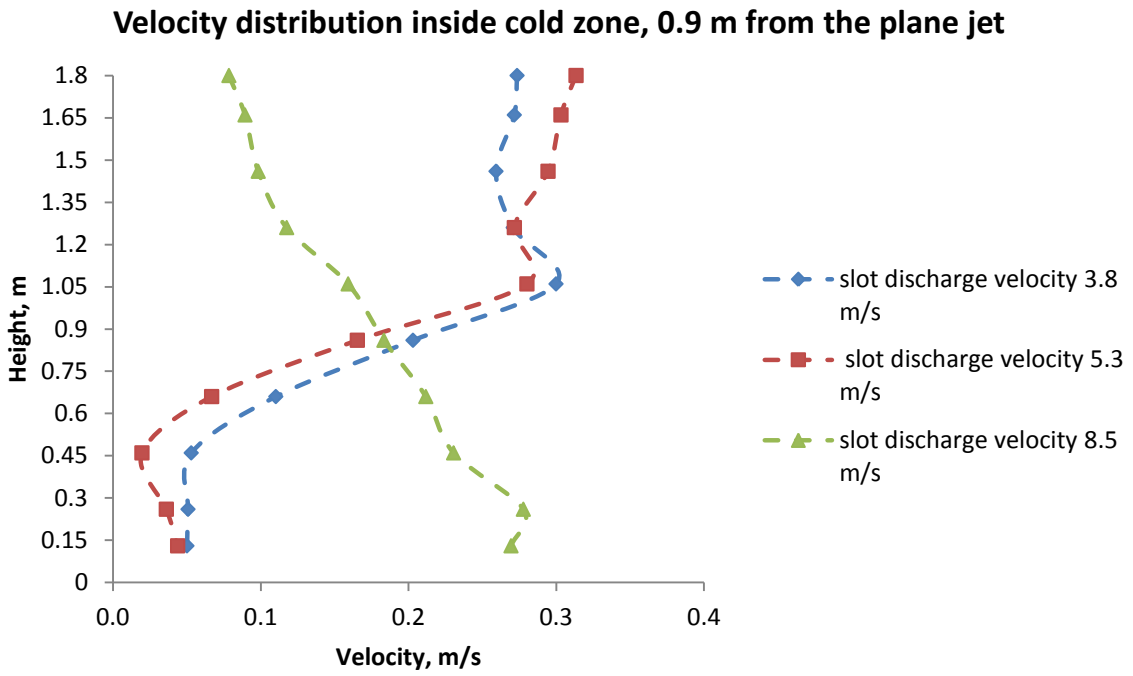

Figure 28. Velocity distribution inside cold zone in the distance of 0.9 m from the plane jet. Blue color refers to discharging velocity from the slot 3.8 m/s, red color refers to velocity 5.3 m/s, green color represent velocity of 8.5 m/s

5.2.2. Case 2: The convector used as a heat source in position *P.1*

In this scenario the convector was placed inside warm zone in order to heat up this zone. Air curtain system remained turned on. Supply velocity from the diffuser was set to 3.8 m/s, 5.3 m/s and 8.5 m/s during the measurements .

5.2.2.1. Temperature distribution

Results of temperature measurements in the distance of 0.9 m from the door aperture inside cold zone are presented in *Table 11*. Again the temperature values are averaged over a ten minutes measurement. *Table 12* summarize results of measured temperature at the same time and inside same zone but for larger distance: 1.8 m from the downward plane jet.

Table 11. Temperature inside cold room at the distance of 0.9 m from the jet.

	Supply velocity		
	3.8 m/s	5.3 m/s	8,5 m/s
Height, m		*Temperature, °C*	
1.8	25.3	27.5	22.5
1.66	25.3	27.5	22.4
1.46	25.7	27.8	22.4
1.26	25.9	27.8	22.5
1.06	25.6	27.5	22.5
0.86	24.6	26.4	22.7
0.66	23.7	25.3	22.9
0.46	22.6	24.7	23.5
0.26	21.7	24.2	23.9
0.13	21.7	24.3	24.1

Table 12. Temperature inside cold room at the distance of 1.8 m from the jet.

	Supply velocity		
	3.8 m/s	**5.3 m/s**	**8,5 m/s**
Height, m		*Temperature, °C*	
2.55	23.8	26.3	22.5
1.95	23.3	25.6	22.2
1.35	22.6	25.2	21.9
0.75	22.0	24.5	21.6
0.15	21.6	24.1	21.2

The values listed in *Table 11* and *Table 12* are shown on *Figure 29* and *Figure 30*. The temperature distribution distant 0.9 m from the jet is presented in *Figure 29*. Again for lower supply velocity the lower temperature values was noted. The similar trend can be seen for supply velocities 3.8 m/s and 5.3 m/s. At level of 0.13 m and 0.26 m similar temperature values were measured. Then temperature started to grow with the altitude. PT-100 sensor located on the level of 1.26 m recorded the highest temperature value. This is comparable to the case when panel heaters were used and supply velocity was 3.8 m/s. Above this point temperature started to decrease.

The temperature distribution for supply velocity 8.5 m/s repeated as in the case with panel heaters. The highest temperature value was recorded at the level of 0.15 m. Temperature decreased with the altitude. For this case the difference between temperature values measured at the lowest and the highest level was the smallest. This difference varies significantly while using convector and panels when discharged velocity is equal to 5.3 m/s. When using panel heaters the difference was 1,2 °C while using convector the difference was 3,2 °C.

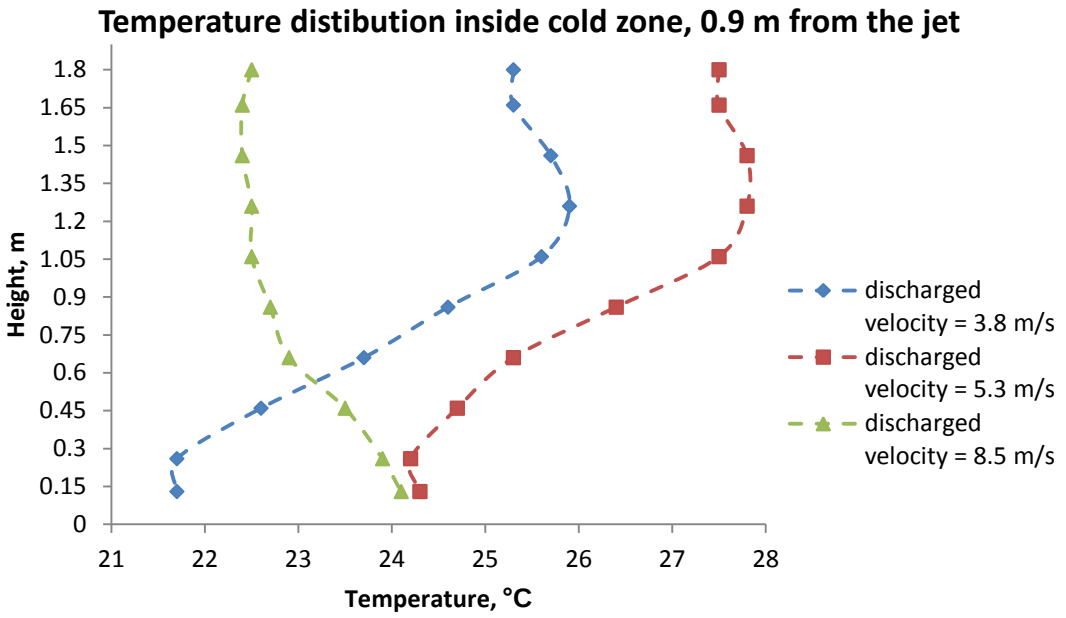

Figure 29. **Temperature distribution inside cold zone in the distance of 0.9 m from the plane jet. Blue color refers to discharging velocity from the slot 3.8 m/s, red color refers to velocity 5.3 m/s, green color represent velocity of 8.5 m/s.**

Results of temperature measured in the distance 1.8 m from the plane jet show highly similar trend for all supply velocities. Again comparison of *Figure 29* and *Figure 30*indicates that with increasing discharged velocity the warm air overcomes longer distance before starting to mix and going upward.

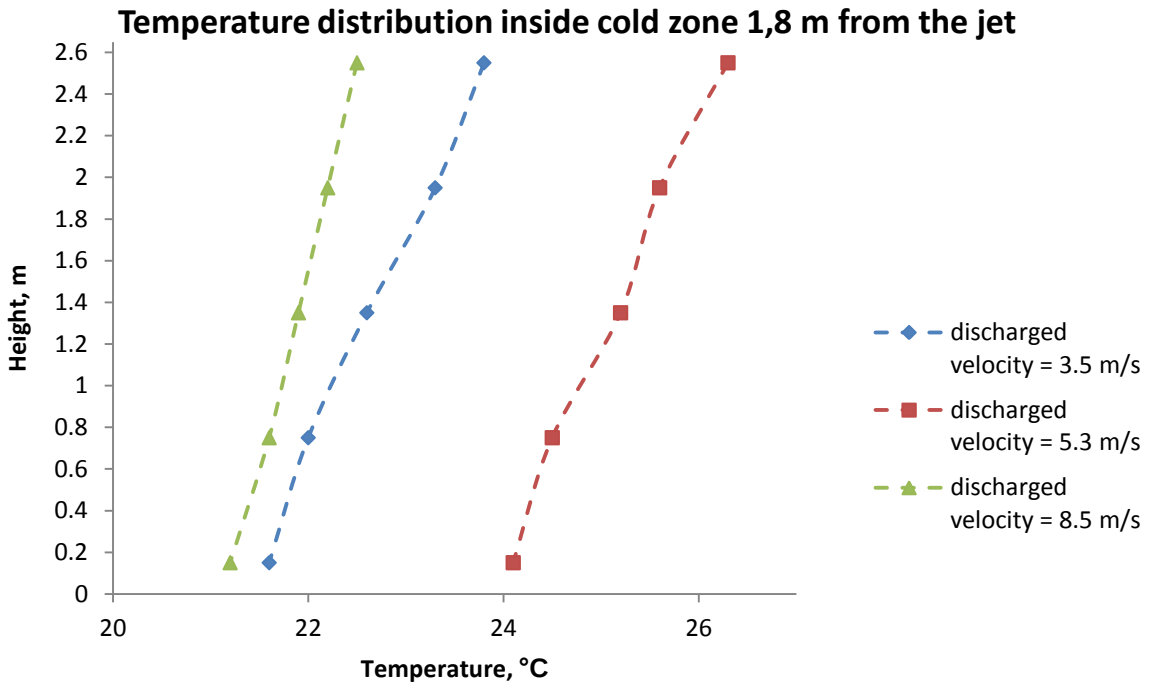

Figure 30. **Temperature distribution inside cold zone in the distance of 1.8 m from the plane jet. Blue color refers to discharging velocity from the slot 3.8 m/s, red color refers to velocity 5.3 m/s, green color represent velocity of 8.5 m/s**

Table 13. Temperature inside warm room at the distance of 1.8 m from the jet. shows the temperature values measured inside warm zone in the distance of 1.8 m from the downward jet. The air temperature distribution is also shown on *Figure 31*.

Table 13. Temperature inside warm room at the distance of 1.8 m from the jet.

	Supply velocity		
	3.8 m/s	**5.3 m/s**	**8,5 m/s**
Height, m	*Temperature, °C*		
2.55	29.0	32.7	29.4
1.95	28.4	31.8	28.6
1.35	26.7	30.2	28.3
0.75	24.3	29.2	27.4
0.15	22.7	28.6	27.2

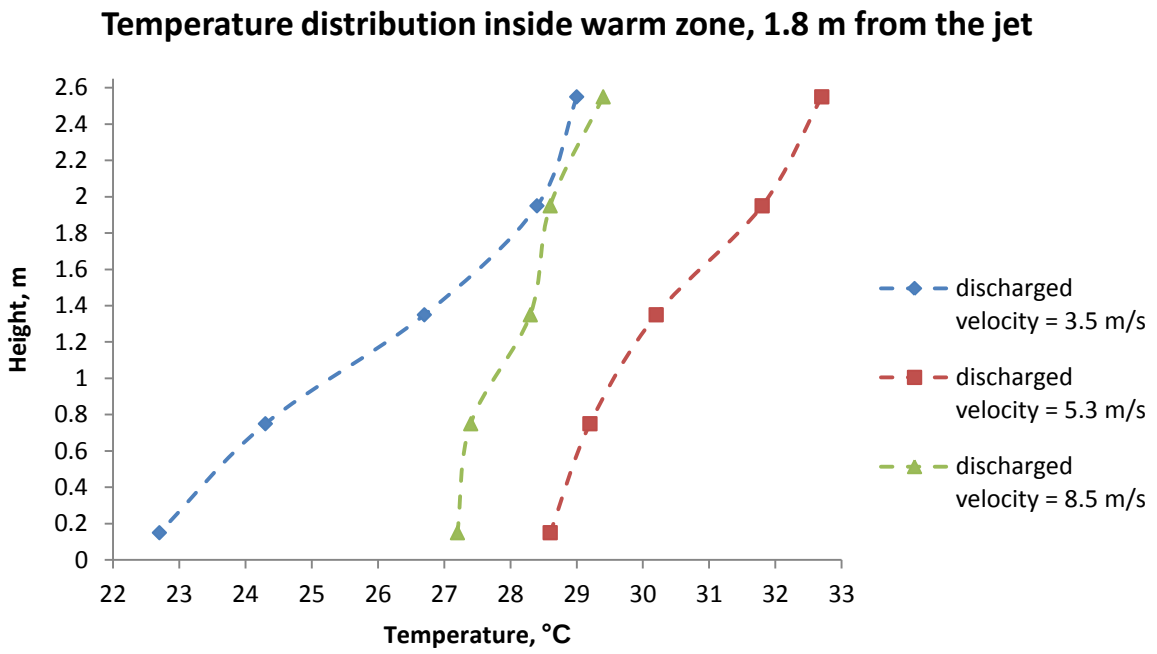

Figure 31. **Temperature distribution inside warm zone in the distance of 1.8 m from the plane jet. Blue color refers to discharging velocity from the slot 3.8 m/s, red color refers to velocity 5.3 m/s, green color represent velocity of 8.5 m/s.**

The temperature distribution inside warm zone is presented in *Table 13* and *Figure 31*. Temperature distribution was highly different for different supply velocities. With increasing the velocity discharged from the slot the warm air inside the warm zone were mixed better and the temperature was more evened at different levels.

5.2.2.2. Velocity distribution

The velocity distribution can be seen on *Figure 32*. The shape of lines which represents slot discharged velocity 3.8 m/s and 5.3 m/s are almost the same. The values measured on each level vary slightly. For both supplied velocities it can be observed that the highest velocity values appeared on the highest levels and decreased slightly downward between level of 1.26 m and 1.86 m from the floor. The lowest values were measured at 0.13 m, 0.26 m and 0.46 m from the floor. Afterwards the velocity increased with the altitude until level of 1.06 m. Between the level of 1.06 m and 1.26 m above the floor velocity decreased insignificantly. Invert trend of velocity distribution is shown for supply velocity equal to 8.5 m/s. The largest

values which was 0.27 m/s were reported at level 0.13 m and 0.26 m. After that while increasing height the velocity decreased uniformly until the value 0.08 m/s.

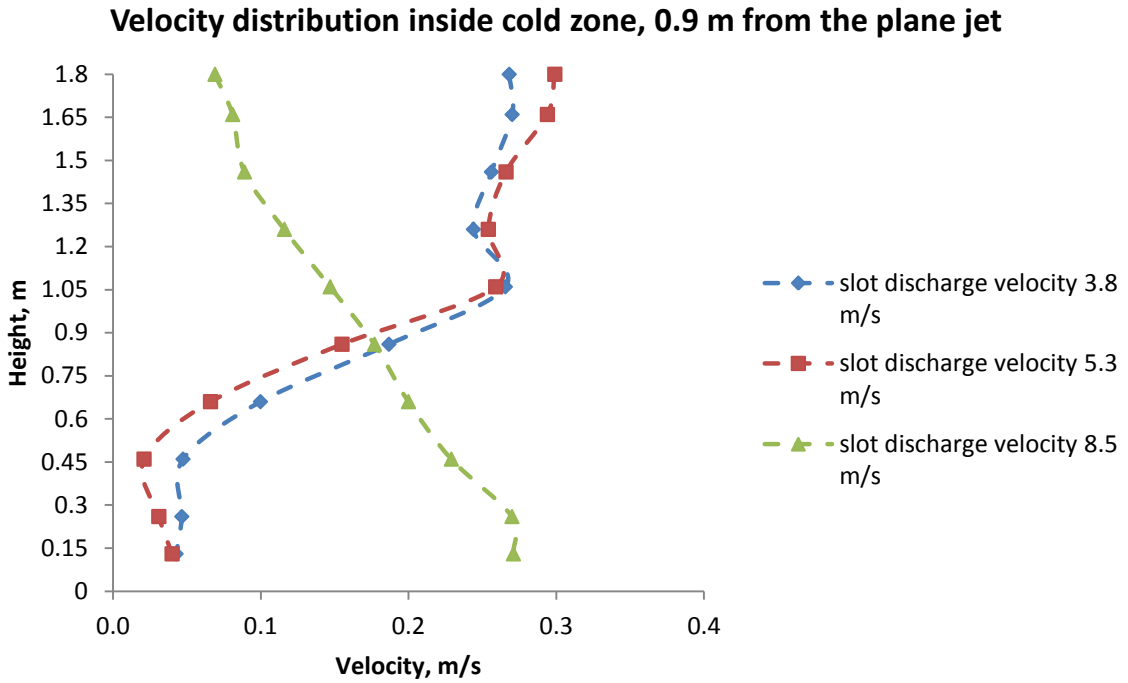

Figure 32. Velocity distribution inside cold zone in the distance of 0.9 m from the plane jet. Blue color refers to discharging velocity from the slot 3.8 m/s, red color refers to velocity 5.3 m/s, green color represent velocity of 8.5 m/s

5.2.3. Discussion

The effect of installing the slot diffuser above the door between two zones was analyzing. One of the zones remained cold while the other zone was warming up by using two different heat sources. First emitted heat more in the radiation way. Second emitted more heat via convection.

Depending on the velocity supplied from the slot diffuser, different performance of the airflow distribution could be observed. Created downward plane jet had visible influence inside both zones. One of the effects was that while increasing discharged velocity less temperature stratification inside both zones could be observed. This is very important conclusion when considering effectiveness of the airflow distribution. In case when the warm air is distributed only as a consequence of density differences, large masses of warm air

occupied top part of the room and it takes a long time to distribute heat to the lower part of the room. This can be seen in Chapter 5.3Series 3: measurements of airflow distribution without using air curtain system. One of the biggest advantages of distributing air with the air curtain system is that the air inside zones is well mixed.

Next effect which comes with increasing velocity supplied with the air curtain system is that it is possible to obtain higher temperature values as well as higher velocity values at lower levels inside cold zone during the continuous work of the air curtain system. That means that it is possible to distribute warm air with the jet into the other room. For the measurements in the distance 0.9 m from the downward plane jet this was achievable only for the highest supply velocity. Therefore it can be assumed that the area occupied by the warm air depends on plane jet parameters, i.e. supply velocity or angle of the jet; and what follows it is dependent also on the geometry of a slot diffuser. Comparing different types of heat source used to heat up the room there were no significant differences between the cases except the temperature stratification in the distance of 0.9 m from the jet when the air was supplied with velocity 5.3 m/s. This may indicate that the heat source type has less impact on the airflow distribution in the room when the air curtain system is used.

The velocity measurements are corresponding to the results of the smoke test presented in Chapter 5.1.1Visualization of the downward plane jet without heater in the room. As was observed for lower supply velocities the air mixed and grew up in the region where the vertical pole were placed which is 0.9 m from the doorway. For supply velocity 8.5 m/s the pole was located before the region where the air mixes and go upward. Therefore the highest velocity was obtained by the bottom probe. The velocity distribution measured inside cold zone confirms the fact that the distributed with the jet air grows up in the distance dependent

on supply velocity. For all cases, values measured at this point did not cross the value of 0.3 m/s what in generally considered as a limit to obtain thermal comfort.

5.3. Series 3: measurements of airflow distribution without using air curtain system.

Third laboratory measurements were conducted without using air curtain system. The airflow was caused only by the density difference of warm and cold air streams inside zones. The temperature and velocity database was collected for three different conditions. In the first test two panel heaters were used as a heat source. Then for the second and third test the heat source was changed for a convector. Detailed description of heating devices parameters and locations are contained in *Internal heating device.*

5.3.1. Case 1: Panel heaters used as the heat source in position *P.1*

Table 14 presents temperature and velocity distribution in the doorway. The values were measured for three different locations. First axis of the door, after that the pole was moved toward left side of the door, 15 cm from the border and then the pole was moved again in a neighborhood of right side, 15 cm from right border. Values presented in *Table 14* are ten minutes averages.

Table 14. Temperature and velocity distribution in the axis of the door and in the distance of 15 cm from the both door vertical borders.

	Axis of the door		*15 cm from the left border of the opening*		*15 cm from the right border of the opening*	
Height [m]	Temperature [°C]	Velocity [m/s]	Temperature [°C]	Velocity [m/s]	Temperature [°C]	Velocity [m/s]
1.8	28.9	0.19	29.1	0.18	28.7	0.22
1.66	28.3	0.15	28.4	0.14	28.0	0.18
1.46	26.1	0.10	26.5	0.10	26.6	0.13
1.26	25.6	0.06	25.9	0.07	26.0	0.08
1.06	25.4	0.05	25.4	0.00	25.7	0.04
0.86	24.5	0.05	24.6	0.07	25.1	0.01
0.66	24.6	0.08	24.7	0.11	25.2	0.05
0.46	24.0	0.11	24.1	0.14	24.6	0.09
0.26	23.8	0.12	23.9	0.17	24.4	0.10
0.13	23.7	0.11	23.8	0.17	24.5	0.08

Temperature distribution measured inside warm and cold zone are summarize in *Appendix 4.*

Temperature distribution inside warm and cold zone while not using air curtain system.

5.3.1.1. Velocity distribution

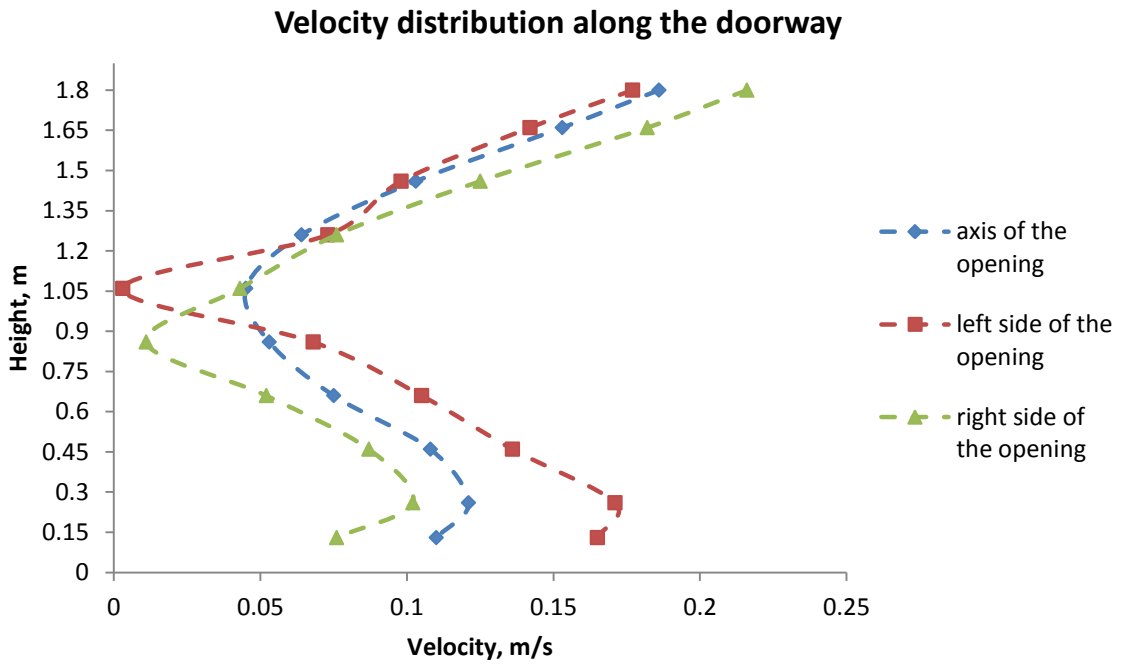

Figure 33. Velocity distribution along the doorway. Blue color indicated velocity values measured in the axis of the aperture. Green and red colors refers to measurement near the right and left borders.

The velocity measurements results are presented in *Figure 33*. The largest velocity values were measured on upper part of the aperture. At the highest level: 1.8 m above the floor noted the highest velocity value for all positions when of the pole moved horizontally. The largest velocity was reported near the right border of the opening and it was 0.216 m/s. Then the velocity decreased with decreasing height of the orifice until level of 1.26 m above the floor. For measurement in the axis of the opening and near its left border the lowest values were measured at level of 1.06 m from the ground and it was 0.45 m/s in the axis, while for left part of the doorway at the same level measured velocity was 0.003 m/s. When the pole was located on the right part of the door, the lowest velocity was noted a bit lower at 0.86 m from the floor, the lowest value was 0.011 m/s. Between 0.26 m and 0.66 m from the floor the velocity decreased with the altitude for all measured position along width of the aperture. The lowest anemometer located at level 0.13 m above the floor measured slightly lower velocity value than on level 0.26 m above the floor. This was repeated for all positions of the pole. The velocity along the whole height of the doorway measured in axis of the opening and on the right and left has different values but general shape of distribution line is similar. The biggest differences was observed in the vicinity of the floor and in the middle of the orifice.

Figure 33 presents directly measured values as the anemometers are not able to measure a direction of the airflow. If we define the direction of the airflow as positive in upper part of aperture where warm air is escaping the warm zone and as negative in lover part of door opening where cold air is entering the warm zone we can convert *Figure 33* for *Figure 34*.

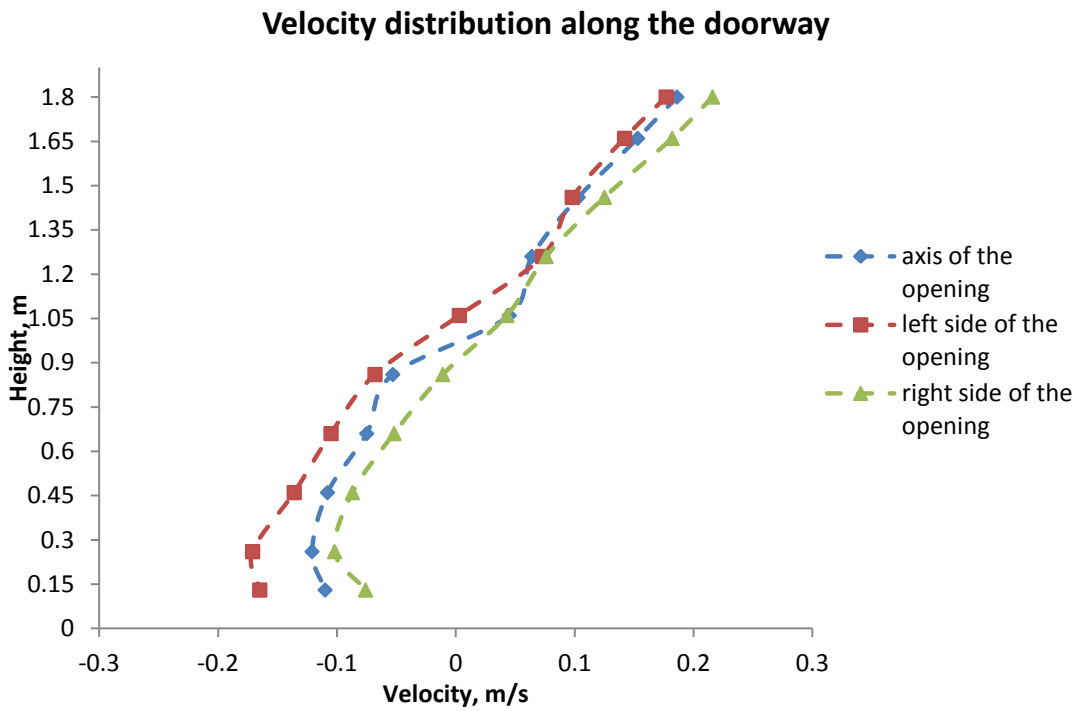

Figure 34. Velocity distribution along the doorway in the axis (blue color) and near right (green color) and left (red color) borders. The graph takes into account the direction of the flow.

Accordingly to literature the velocity in upper part of the doorway should have approximately the same values as in bottom part. In the middle of the doorway neutral plane should be located so the velocity should fluctuate slightly around zero.

5.3.1.2. Temperature distribution

Figure 35 shows temperature distribution measured along the doorway. Temperature distribution was measured for three different position in the orifice. There were no significant changes where the pole was moved in different position along the width of the aperture. Therefore *Figure 35* present only temperature distribution in the axis of the doorway. Upper temperature sensors reported warmer air temperature values. The highest located probe measured the warmest value. The lower sensors measured temperature similar to temperature inside cold zone while upper sensors measured temperature values similar to temperature inside warm zone. This can be seen in *Figure 36*. Accordingly to the theory, there should be visible gap between upper and lower air temperature values. This should indicate clear

division into two streams of air with varying temperature values. This is not the case here. Temperature values on a graph above between level of 0.75 m above the floor and 1.35 may indicate that in the middle of the door and in its vicinity the streams of warm and cold air were mixing.

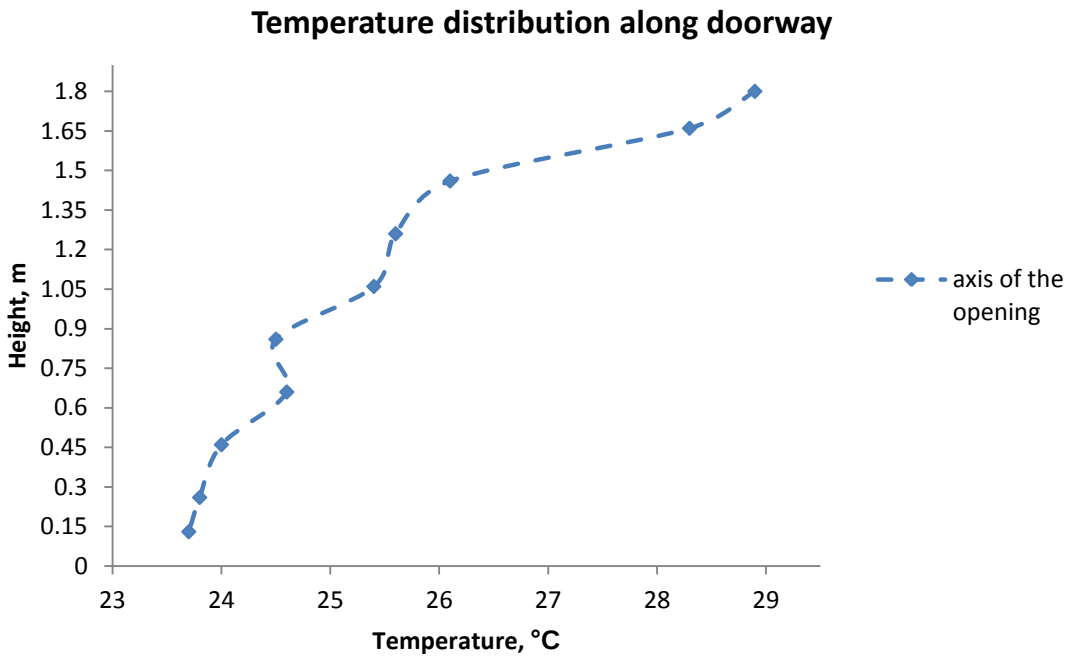

Figure 35. Temperature distribution along the doorway measured in the axis of the opening.

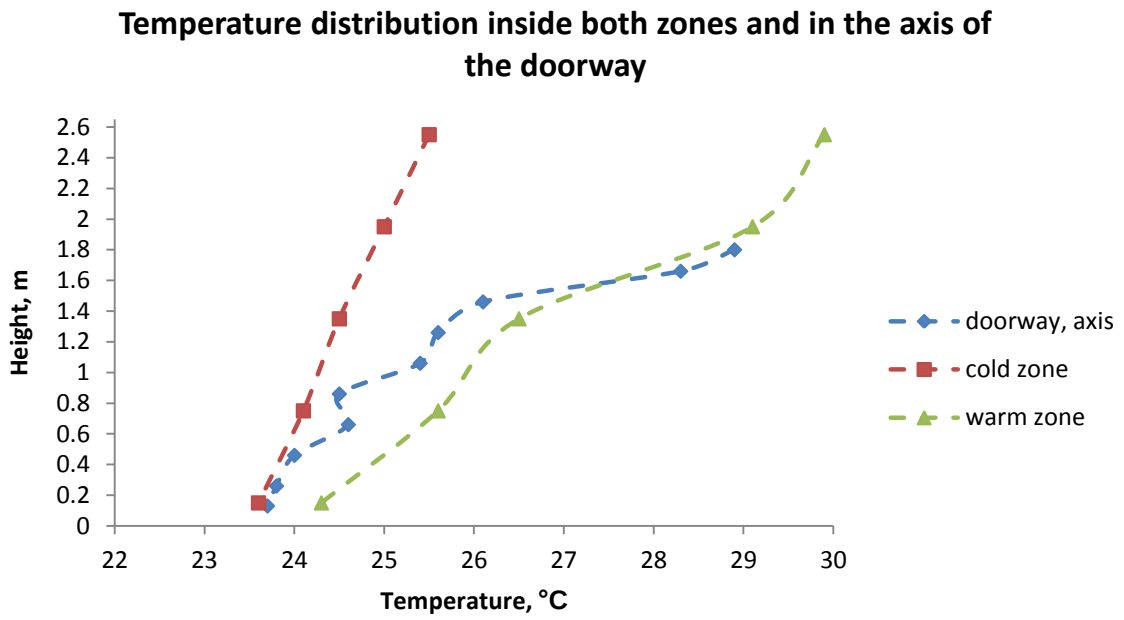

Figure 36. Temperature distribution inside cold zone (red color), warm zone (green color) measured in the distance of 1.8 m from the door opening. Velocity distribution in the axis of the door opening is market in blue.

Temperature distribution inside warm and cold zone is different. In both zones upper part of zone remained warm while in the lower part of zone lower temperature values were observed. Differences between temperature near the ceiling and near the floor were much larger inside warm zone and reached up even 5.5°C. Inside cold zone temperature difference between the highest and the lowest located sensors was 1.9°C.

5.3.2. Case 2: The convector used as a heat source in position *P.1*

Table 15 presents temperature and velocity distribution in the doorway measured when the convector located in position *P.1* were used as a heat source. Again the values were measured for three different locations so the pole was moved manually in the same positions as in Case 1. Values are presented in *Table 15* are ten minutes averages.

Table 15. Temperature and velocity distribution in the axis of the door and in the distance of 15 cm from the both door vertical borders.

	Axis of the door		*15 cm from the left border of the opening*		*15 cm from the right border of the opening*	
Height [m]	Temperature [°C]	Velocity [m/s]	Temperature [°C]	Velocity [m/s]	Temperature [°C]	Velocity [m/s]
1.8	28.8	0.25	29.8	0.27	30.9	0.29
1.66	28.5	0.22	29.6	0.21	30.8	0.27
1.46	27.3	0.19	28.9	0.16	30.3	0.24
1.26	24.1	0.05	25.2	0.05	25.6	0.03
1.06	22.9	0.05	23.9	0.07	24.9	0.04
0.86	22.5	0.05	23.5	0.08	24.6	0.03
0.66	22.4	0.07	23.3	0.12	24.3	0.06
0.46	21.9	0.10	22.8	0.13	23.7	0.09
0.26	21.7	0.09	22.5	0.16	23.5	0.09
0.13	21.7	0.08	22.5	0.17	23.4	0.07

Temperature distribution measured inside warm and cold zone are summarize in *Appendix 4. Temperature distribution inside warm and cold zone while not using air curtain system.*

5.3.2.1. Velocity distribution

Figure 37 shows velocity distribution along the doorway. The velocity presented on the graph has defined direction. The minus values refer to air which enters the warm zone, the plus values concern air which was escaping the warm zone. The measured values in different position vary mainly at lower part of the doorway, between 0.13 m and 0.86 m of the height. Velocity in axis and right side of the aperture were almost the same but on the left side of the opening, the lower values at level of: 0.13 m, 0.26 m. 0.46 m, 0.66 m and 0.86 m were recorded. The largest difference which was 0.1 m/s was noted at level of 0.13 m above the floor. For all measured locations of the pole the lower part values were smaller. The difference between the highest and the lowest located probe was 1,69 m/s in the axis of the door, while on the left side of the door is was 0,097 m/s. There is a big gap between values measured at level 0.86 m and 1.06 m. It can be assumed that the neutral plane is located in between of these heights. In the upper part of the aperture the velocity values were more

similar in the axis and on the left side. The highest velocities were measured on the right side of the doorway.

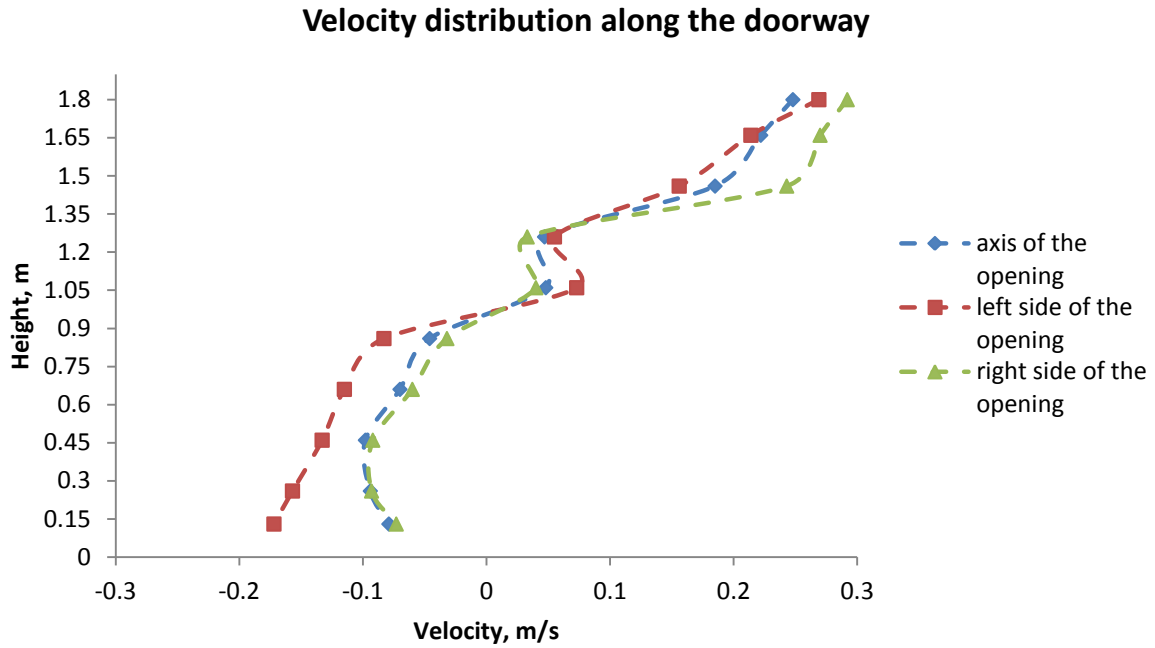

Figure 37. Velocity distribution along the doorway in the axis (blue color) and near right (green color) and left (red color) borders. The graph takes into account the direction of the flow.

5.3.2.1. Temperature distribution

Results of temperature measurements can be seen in *Figure 38*. There were clear distinction between warm and cold air. The warmest air filled upper part of the aperture and the highest temperature value was measured at height 1.8 m. The gradient of 3.2 °C between 1.26 m and 1.46 m above the floor was observed. The temperature distribution fits more to the theory than in the previous case while using the panel heaters. The difference between the lowest and the highest probe was 7.1 °C. It can be seen that even after the time of three hours of warming up the room, stratification was large and masses of warm air remained in the upper part of the room very close to the doorway.

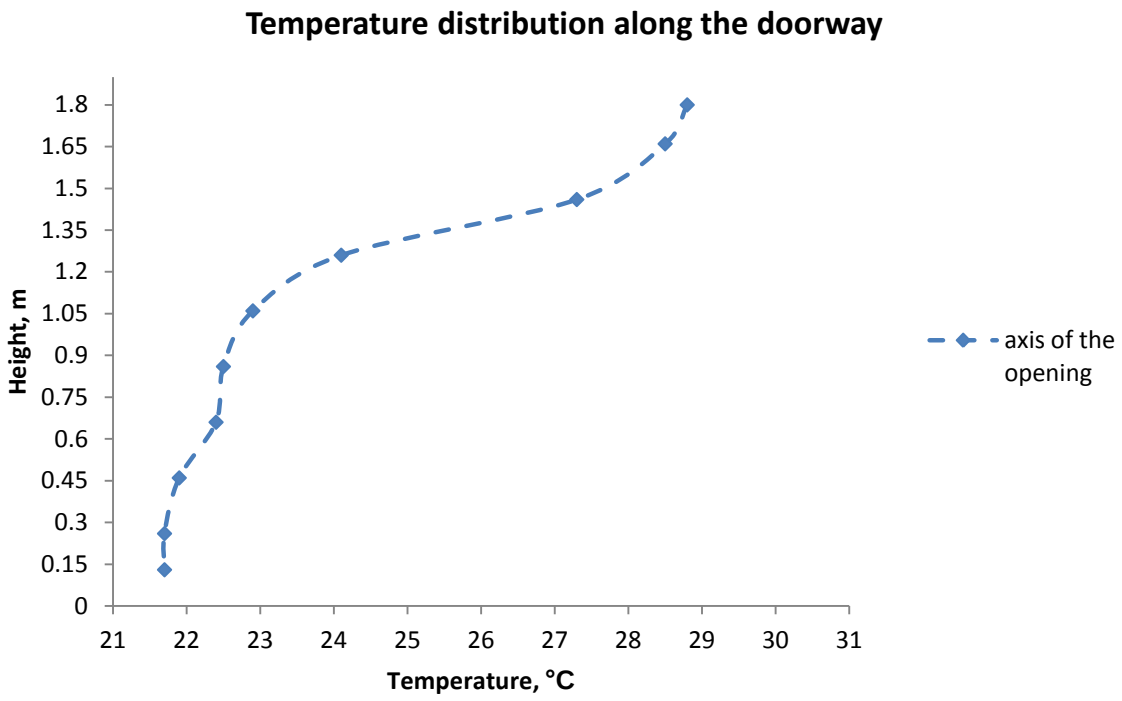

Figure 38. Temperature distribution along the doorway measured in the axis of the opening.

Temperature distribution inside warm and cold zone presents following: in both zones upper part of zone remained warm. In the lower part of zone the lowest temperature values were observed. However the larger temperature stratification can be observed in the aperture and inside warm zone.

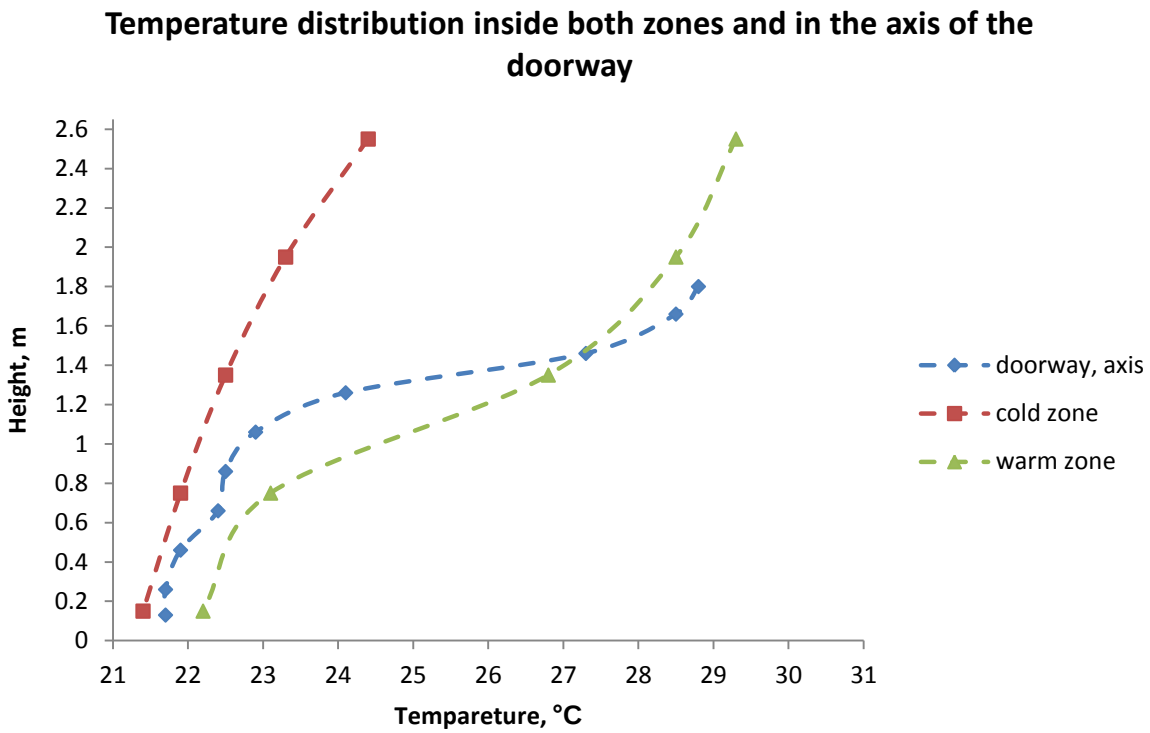

Figure 39. Temperature distribution inside cold zone (red color), warm zone (green color) measured in the distance of 1.8 m from the door opening. Velocity distribution in the axis of the door opening is market in blue.

5.3.3. Case 3: The convector used as a heat source in position *P.2*

This case has been conducted in order to check if the position of the heat source has impact on airflow distribution inside zones and in the axis of the doorway. Therefore the convector was placed in position P.2 (see Figure 7). The rest of parameters did not changed, however it is needed to remember that initial temperature varied a little in each case. Temperature distribution measured inside warm and cold zone are summarize in *Appendix 4. Temperature distribution inside warm and cold zone while not using air curtain system. Table 16* contains the results of measurements of three different positions in doorway.

Table 16. Temperature and velocity distribution in the axis of the door and in the distance of 15 cm from the both door vertical borders.

	Axis of the door		*15 cm from the left border of the opening*		*15 cm from the right border of the opening*	
Height [m]	Temperature [°C]	Velocity [m/s]	Temperature [°C]	Velocity [m/s]	Temperature [°C]	Velocity [m/s]
1.8	29.6	0.294	30.4	0.302	31.3	0.317
1.66	28.9	0.251	30.0	0.243	30.4	0.287
1.46	28.2	0.164	29.0	0.175	28.6	0.178
1.26	24.7	0.064	25.4	0.062	25.9	0.050
1.06	23.9	0.046	24.4	0.050	25.4	0.011
0.86	23.6	0.053	24.0	0.068	25.1	0.040
0.66	23.6	0.081	24.2	0.099	24.9	0.065
0.46	22.9	0.106	23.4	0.134	24.2	0.100
0.26	22.8	0.120	23.0	0.149	24.0	0.100
0.13	22.7	0.115	23.1	0.165	24.1	0.100

5.3.3.1. Velocity distribution

The velocity distribution is presented in *Figure 40*. The negative values refer to movement of cold air which enter the hot zone, positive values are related to movement of warm air which was escaping the warm room. Comparing this graph with Figure 37 which represents position *P.1* of heat source, it can be observed that the distribution in both cases has similar trend. Velocity profile measured at the different positions along the width of the doorway also displays similar shapes. Again higher differences can be observed at the lowest level. Then the lines go parallel until height of 1.06 m above the floor. The lowest velocities for all location of the pole were measured between 0.86 m and 1.06 m above the floor. It can be assumed that the neutral plane was located somewhere between those heights. It can be also assumed that the location of heat source has no influence of the airflow distribution while the air movement are not interrupted by any other factors.

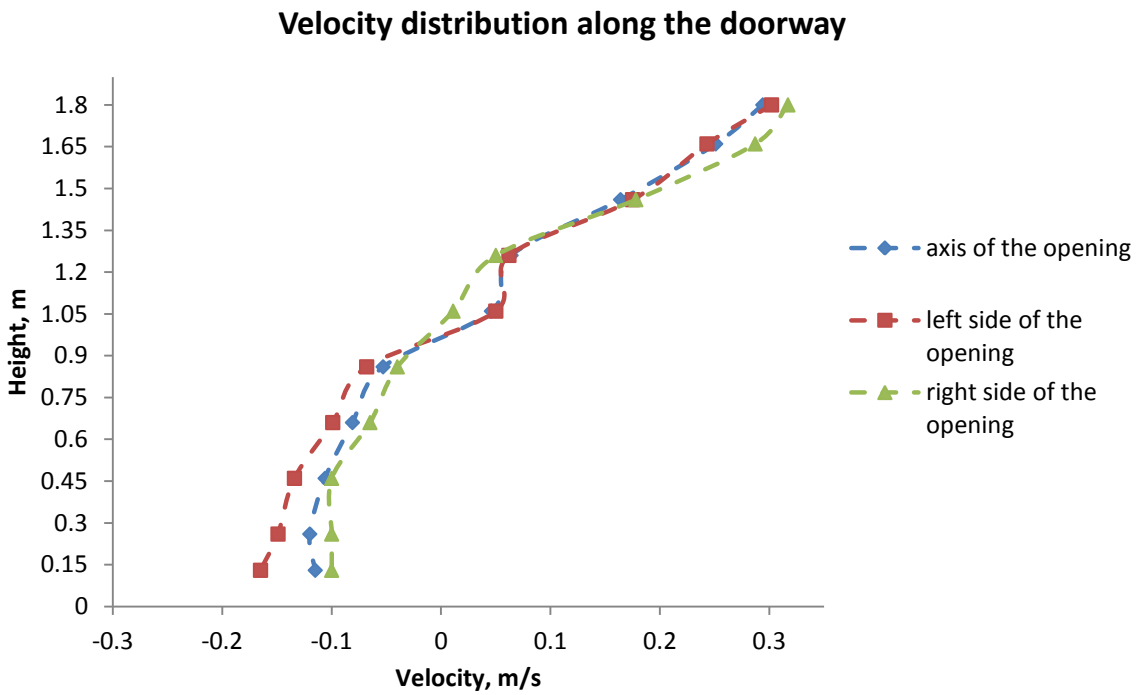

Figure 40. Velocity distribution along the doorway in the axis (blue color) and near right (green color) and left (red color) borders. The graph takes into account the direction of the flow.

5.3.3.1. Temperature distribution

Figure 41 and *Figure 42* present results of temperature measurements along the doorway and inside both zones. There were no significant differences while moving the pole horizontally, therefore the graph contains only the temperature values measured in axis of the doorway. Distinction between warm and cold air could be seen. The warm air remained in the upper part of the aperture and the highest temperature, 29,6 °C was measured at height 1.8 m. There was a change of 3.5 °C between 1.26 m and 1.46 m above the floor. The temperature difference between the lowest and the highest probe was 6,7 °C. The line on the graph has similar shape as the line on *Figure 38* presented for previous case.

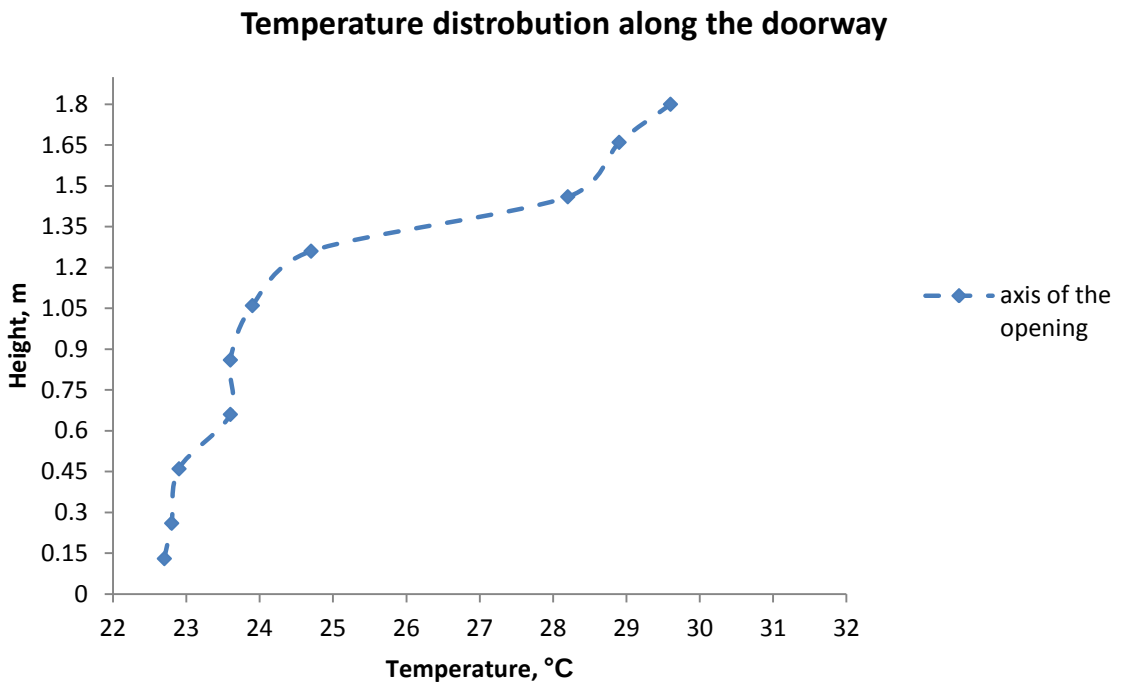

Figure 41. Temperature distribution along the doorway measured in the axis of the opening.

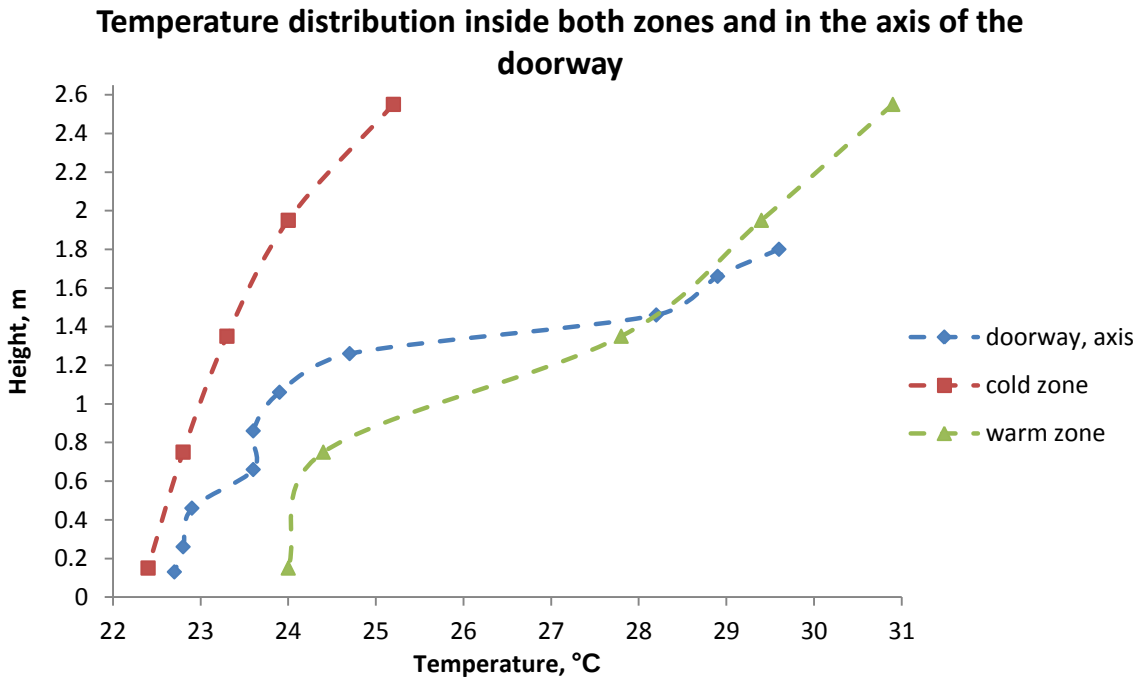

Figure 42. Temperature distribution inside cold zone (red color), warm zone (green color) measured in the distance of 1.8 m from the door opening. Velocity distribution in the axis of the door opening is market in blue.

5.3.4. Visualization of bidirectional airflow through doorway

In order to visualize the bidirectional airflow through the door opening the air with smoke was supplied with the pipe directly into warm room. The smoke was discharged with vertical direction of flow near the place where source of heating was placed. The test was conducted under the steady-state, the room was warm up before. Supplied smoke mixes with warm room air and followed its movement. In *Figure 43* the smoke supply pipe was marked with red arrow. Black arrow pointed the discharging place.

Figure 43. The warm zone filled with the smoke during the smoke test operation. Discharging point is marked with black arrow.

In a time of about 3 minutes the smoke filled upper part of the room and started to escape the room through door opening. *Figure 44 a), b), c)* and *d)* present the view taken from cold zone. Red arrows indicates the warm air movement. The flow of cold air entering the warm

zone was marked in blue. In the middle part of door opening both streams – warm and cold air – mixes. This can be seen in *Figure 44 b), c)* and *d)* and was marked white arrows.

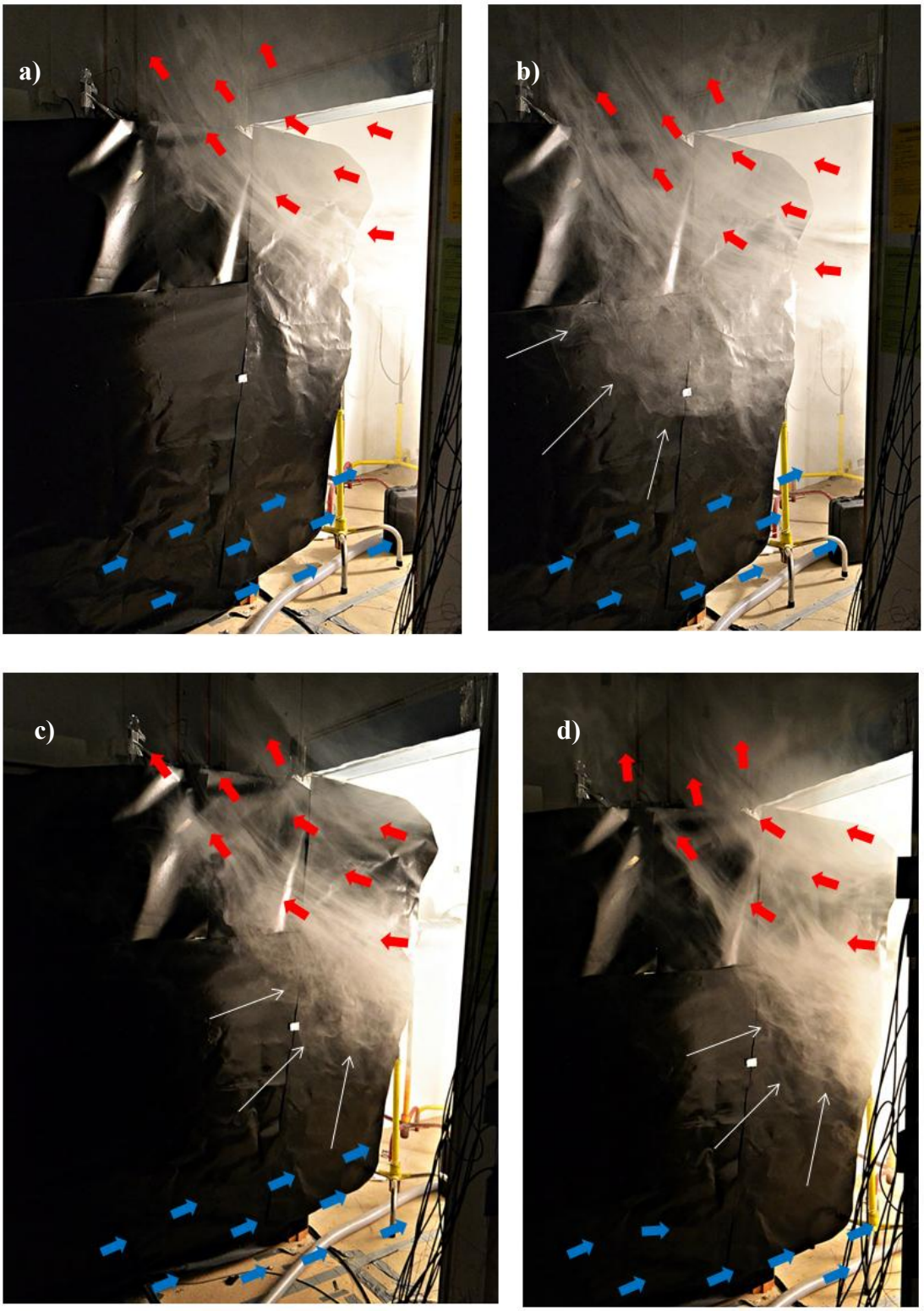

Figure 44. The bi-directional air flow throught the door opening. Red arrows ilustarate warm air distribution. Blue arrows present the cold air movement. The mixing of two streams is pointed with white arrows.

5.3.5. Discussion

In this experimental part bidirectional airflow through door opening was observed. This method of the heat distribution, which is a consequence of the airflow distribution, is considered as a passive heat distribution. All conducted measurements showed similar airflow distribution both inside cold and warm zone. The warm air cumulate in the upper part of the rooms while cold air took lower part. The velocity profiles follow the same shape as the theoretical velocity profile, but with many deviations which make the velocity profiles based on the measurements asymmetric.

The neutral plane while operate with panel heaters was hard to find based on temperature profiles. Additionally the smoke test results display the mixing of the air between warm and cold streams, which appeared in middle of the door opening. Previous investigations of (Georges et al. 2013) assumed no mixing between the air streams. This was not a case in the conducted measurements. The reason could be that the steady-state regime may not achieved during the experiment or it could also be caused by too high temperature differences between zones.

The type of the heating device appears to have an impact on the airflow distribution inside zones. Emitting the heat from panel heater seem to support decreasing of temperature stratification. Moreover, lower velocity values were obtained in case when panel heaters were used. Changing the position of the heating device had no significant influence on the indoor airflow distribution. Both temperature and velocity profiles display highly similar shape. There was no significant differences neither when the pole was moved horizontally. This results confirm the assumption of uniform temperature and velocity distribution along the whole width of the door opening.

Warming up one zone inside the building while leaving the rest of rooms unheated may lead to huge temperature differences both within and between zones.

6. Conclusions and future work

The integration of wood stoves in low-energy buildings has meet many challenges regarding emissions, efficiencies and the transient heat release from combustion of wood. It may be assumed that one wood stove may provide heat into the entire building. However, this assumption require further investigations for the reason that some aspects such as indoor air quality of nZEB using stoves remains unclear.The conclusions are made on the basis of the results of the airflow distribution measurements inside the zone where the space heating device was placed as well as inside the unheated zone connected with the warm zone.

The reference case represents the passive method of heat distribution and for this case the following phenomenon has been observed: the warm air cumulates in the upper part of the warm zone while cold air occupied the lower part of the warm zone. This leads to vertical temperature differences inside zones. For cold zone the stratification varies from 1,9°C to 3,1°C. For warm zone the stratification was between 5,5°C (for panel heater in position *P.1*) and 7,1°C (for the convector in position *P.1*) . Moreover, depending on geometry of the building, there is a risk that the room equipped with stove may be overheated while the rest of the building may not obtain enough amount of energy to be heated up. The airflow profiles, based on the velocity measurements, show parabolic shape and it was correspondent to theoretical assumptions. However some mixing between warm and cold stream in the middle of the door opening was observed. This was observed when the convector were used as the heat source. Therefore it can be concluded that the type of the heating device have an impact on the airflow distribution inside warm zones. Emitting the heat from panel heater seem to support decreasing of temperature stratification and generate lower velocity values in the door opening. However, changing the position of the heating device seems to have no significant influences on the indoor airflow distribution. No significant differences were noticed neither when the pole was moved horizontally.

This thesis presents a new method of heat distribution which combines passive and active methods of heat distribution. The experimental results show that the air distributed by the slot diffuser would provide better mixing inside both zones and minimize vertical temperature differences inside zones. The stratification inside cold zone varies between 1.8°C(for discharged velocity 3.8 m/s) and 1°C (for discharged velocity 8.5 m/s). The temperature stratification inside warm zone varies between 5,2°C (for discharged velocity 3.8 m/s) and 1.8°C (for discharged velocity 8.5 m/s). Comparing to the temperature stratification reached when not using air curtain system it can be concluded that distributing air with the slot diffuser located above the doorway decreases vertical temperature stratification inside both zones. Moreover, supplying the warm air through the air curtain system decreases the period of time needed to achieve the uniform thermal environment inside the whole building. The discharge velocity of downward plane jet from the slot diffuser directly affect the performance of the airflow distribution between zones. When the discharged velocity equals to 8.5 m/s, the temperature gradient inside both zones was decreased. This may be an important note regarding the effectiveness of the airflow distribution.

In addition increasing the discharged velocity of the downward jet may increase the air temperature at lower part of the cold zone during the period of running the air curtain system.. Comparing the performance of heat distribution by using different types of heat source used to heat up the room, there were no significant differences between these cases. This may indicate that the heat source type has limited impact on the heat distribution and airflow distribution between zones in the room when the air curtain system is used. In practice, improperly designed air curtain system may have negative impact on heat transfer between zones.

There are some practical limitations in the presented study. Future work may be carried out to get better understanding of the new method of heat distribution and airflow distribution.

- Generally speaking, the air curtain systems are designed and used to limit the heat and mass transfer between zones with different parameters. In order to avoid this situation the integration of air curtain system and heating system require further investigation i.e. the discharging angle of downward jet may be changed.
- There is a lack of temperature measurements along the jet and velocity profiles inside both zones. These measurements may help to understand the detailed airflow distribution inside zones. Further study may focus on the thermal comfort issues inside both zones.
- The experimental measurements were conducted by using different supply air velocity (from 3.8 m/s to 8.5 m/s) from the slot diffuser. As the discharge velocity will affect the performance of heat distribution, it is therefore interesting to investigate the airflow distribution with discharged velocity in the range 5.3 – 8.5 m/s.

Bibliography

[1] Agency, I. E. (1992). Annex 20 Air Flow Patterns within Buildings, Airflow through large openings in buildings.
(2013). *Air Velocity Transducer 8455/8465/8475.* TSI, Editor.

[2] Allen, R., Leckie, S., Millar, G., & M, B. (2009). The impact of wood stove technology upgrades on indoor residential air quality. W *Atmospheric Environment 43* (strony 5908-5915). Elsevier.

[3] Atanasiu, B. (2011). *Principles for nearly-zero energy buildings.* Buildings Performance Institute Europe.

[4] Awbi, H. B. (1998). Energy Efficient Room Air Distribution. W *Renewable Energy 15* (strony 293-299). Elsevier.

[5] Bugge, M., Skreiberg, Ø., Seljeskog, M., & Lundquist, A. (2014). StableWood. New solutions and technologies for heating of buildings with low heating demand:Stable heat release and distribution from batch combustion of wood. Trondheim.

[6] Cao, G. (2009). *Modelling the attached plane jet in a room.* Espoo.

[7] Cao, G., & et al. (2011). Protected zone ventilation for reducing personal exposure to indoor pollutants. *Indoor Air Conference.*

[8] Cao, G., Kandziab, C., Müllerb, D., & Heikkinena, J. (2013). Experimental study of the effect of turbulence intensities on the maximum velocity decay of an attached plane jet. W *Energy and Building 65* (strony 127-136). Elsevier.

[9] Carvalho, R., Jensen, O., Afshari, A., & Bergsøe, N. (2013). Wood-burning stoves in low-carbon dwellings. W *Energy and Buildings 59* (strony 244-251). Copenhagen: Elsevier.

[10] Essel, E. E., F, T. M., Agelin-Chaab, M., Koupriyanov, M., & Tully, B. (2013). Particle image velocimetry measurements in curved turbulent. W *Experimental Thermal and Fluid Science 49* (strony 169-184).

[11] Eurostat. (2006-2007). Europe in figures. Eurostat yearbook 2006-7. European Comission.

[12] Frank K. Lu, A. J. (2008). Visualising the flow inducted by an air curtain using stereo particle image velocimetry. *ISFV13 - 13th International Symposium on Flow Visualization.* Nice, France.

[13] Georges, L., & Mathises, H. M. (2015). Convective Heat Transfer between Rooms in Nordic Passive Houses.

[14] Georges, L., Skreiberg, Ø., & Novacovic, V. (2014). On the proper integration of wood stoves in passive houses undercold climates. W *Energy and Buildings 72* (strony 87-95). Trondheim: Elsevier.

[15] Georges, L., Skreiberg, Ø., & Novakovic, V. (2013). On the proper integration of wood stoves in passive houses: Investigation using detailed dynamic simulations. W *Energy and Buildings 59* (strony 203-213). Elsevier.

[16 International Energy Agency. (1992). Annex 20 Air Flow Patterns within Buildings, Airflow through large openings in buildings.
[17] Krajewski, G. (2013). Efficiency of air curtains used for separating smoke free zones in case of fire. Chambery.
[18] Kunkel, S., & Kontonasiou, E. (brak daty). *Indoor air quality, thermal comfort and daylight policies on the way to nZEB – status of selected MS and future policy recommendations.* Pobrano z lokalizacji http://bpie.eu/.
[19] Mathisen, H. M., & Georges, L. (2015). Convective Heat Transfer between Rooms in Nordic Passive Houses. W . .
[20] Pettersen, M. (2014). Thermal comfort with simplified heat distribution systems in highly insulated buildings.
[21] Q. Liu, S. J. (1996). COMPARISON OF THREE k-e TURBULENCE MODELS. American Society of Agriculmral Engineers 0001-2351 / 96 / 3902-0689.
[22] Schlichting, H. (1979). *Boundary-Layer Theory.* New York: McGRAW-HILL BOOK COMPANY.
[23] Skistad, H. (1995). *Industriventilasjon. Innblåsning og avsug. Teorigrunnlag for beregning av isoterme stråler og avsug.* Oslo: Skarland Press AS.
[24] Skreiberg, Ø., & Karlsvik, E. (2011). ACHIEVING LOW EMISSIONS AND STABLE HEAT RELEASE FROM WOOD STOVE S AND FIREPLACES FIRING AT LOW LOAD.
[25] Torcellini, P., Pless, S., Deru, M., & Crawley, D. (2006). Zero Energy Buildings: A Critical Look at the Definition. *ACEEE Summer Study.* California.
[26] Toscano, G., Duca, D., Amato, A., & Pizzi, A. (2014). Emission from realistic utilization of wood pellet stove. W *Energy 68* (strony 644-650). Elsevier.

Figure and table list

Figure list:

Table list:

Appendix 1: Calibration of velocity probes.

A3.1 Calibration of probe 43

Velocity set in the tunnel	*Value measured with probe 43*	*±3.0% of reading*	*±1.0% of selected full scale range*	*Total error*	*Minimum value*	*Maximum value*
m/s	m/s	m/s	m/s	m/s	m/s	m/s
0.200	0.212	0.00636	0,025	0.03136	0.18064	0.24336
0.400	0.411	0.01233	0,025	0.03733	0.37367	0.44833
0.600	0.621	0.01863	0,025	0.04363	0.57737	0.66463
0.800	0.864	0.02592	0,025	0.05092	0.81308	0.91492
1.000	1.079	0.03237	0,025	0.05737	1.02163	1.13637

A3.2 Calibration of probe 47

Velocity set in the tunnel	*Value measured with probe 47*	*±3.0% of reading*	*±1.0% of selected full scale range*	*Total error*	*Minimum value*	*Maximum value*
m/s	m/s	m/s	m/s	m/s	m/s	m/s
0.200	0.205	0.00615	0,025	0.03115	0.17385	0.23615
0.400	0.407	0.01221	0,025	0.03721	0.36979	0.44421
0.600	0.644	0.01932	0,025	0.04432	0.59968	0.68832
0.800	0.922	0.02766	0,025	0.05266	0.86934	0.97466
1.000	1.133	0.03399	0,025	0.05899	1.07401	1.19199

A3.3 Calibration of probe 45

Velocity set in the tunnel	*Value measured with probe 45*	*±3.0% of reading*	*±1.0% of selected full scale range*	*Total error*	*Minimum value*	*Maximum value*
m/s	m/s	m/s	m/s	m/s	m/s	m/s
0.200	0.206	0.00618	0,025	0.03118	0.17482	0.23718
0.400	0.38	0.01140	0,025	0.03640	0.34360	0.41640
0.600	0.557	0.01671	0,025	0.04171	0.51529	0.59871
0.800	0.813	0.02439	0,025	0.04939	0.76361	0.86239
1.000	0.984	0.02952	0,025	0.05452	0.92948	1.03852

A3.4 Calibration of probe 37

Velocity set in the tunnel	*Value measured with probe 37*	*±3.0% of reading*	*±1.0% of selected full scale range*	*Total error*	*Minimum value*	*Maximum value*
m/s	m/s	m/s	m/s	m/s	m/s	m/s
0.200	0.201	0.00603	0,025	0.03103	0.16997	0.23203
0.400	0.364	0.01092	0,025	0.03592	0.32808	0.39992
0.600	0.549	0.01647	0,025	0.04147	0.50753	0.59047
0.800	0.755	0.02265	0,025	0.04765	0.70735	0.80265
1.000	0.901	0.02703	0,025	0.05203	0.84897	0.95303

A3.5 Calibration of probe 46

Velocity set in the tunnel	*Value measured with probe 46*	*±3.0% of reading*	*±1.0% of selected full scale range*	*Total error*	*Minimum value*	*Maximum value*
m/s	m/s	m/s	m/s	m/s	m/s	m/s
0.200	0.231	0.00693	0,025	0.03193	0.19907	0.26293
0.400	0.46	0.01380	0,025	0.03880	0.42120	0.49880
0.600	0.735	0.02205	0,025	0.04705	0.68795	0.78205
0.800	1.02	0.03060	0,025	0.05560	0.96440	1.07560
1.000	1.276	0.03828	0,025	0.06328	1.21272	1.33928

A3.6 Calibration of probe 39

Velocity set in the tunnel	*Value measured with probe 39*	*±3.0% of reading*	*±1.0% of selected full scale range*	*Total error*	*Minimum value*	*Maximum value*
m/s	m/s	m/s	m/s	m/s	m/s	m/s
0.200	0.209	0.00627	0,025	0.03127	0.17773	0.24027
0.400	0.433	0.01299	0,025	0.03799	0.39501	0.47099
0.600	0.642	0.01926	0,025	0.04426	0.59774	0.68626
0.800	0.908	0.02724	0,025	0.05224	0.85576	0.96024
1.000	1.171	0.03513	0,025	0.06013	1.11087	1.23113

A3.7 Calibration of probe 38

Velocity set in the tunnel	*Value measured with probe 38*	*±3.0% of reading*	*±1.0% of selected full scale range*	*Total error*	*Minimum value*	*Maximum value*
m/s	m/s	m/s	m/s	m/s	m/s	m/s
0.200	0.205	0.00615	0,025	0.03115	0.17385	0.23615
0.400	0.365	0.01095	0,025	0.03595	0.32905	0.40095
0.600	0.652	0.01956	0,025	0.04456	0.60744	0.69656
0.800	0.798	0.02394	0,025	0.04894	0.74906	0.84694
1.000	0.971	0.02913	0,025	0.05413	0.91687	1.02513

A3.8 Calibration of probe 53

Velocity set in the tunnel	*Value measured with probe 53*	*±3.0% of reading*	*±1.0% of selected full scale range*	*Total error*	*Minimum value*	*Maximum value*
m/s	m/s	m/s	m/s	m/s	m/s	m/s
0.200	0.186	0.00558	0,025	0.03058	0.15542	0.21658
0.400	0.364	0.01092	0,025	0.03592	0.32808	0.39992
0.600	0.572	0.01716	0,025	0.04216	0.52984	0.61416
0.800	0.872	0.02616	0,025	0.05116	0.82084	0.92316
1.000	1.106	0.03318	0,025	0.05818	1.04782	1.16418

A3.9 Calibration of probe 40

Velocity set in the tunnel	*Value measured with probe 40*	*±3.0% of reading*	*±1.0% of selected full scale range*	*Total error*	*Minimum value*	*Maximum value*
m/s	m/s	m/s	m/s	m/s	m/s	m/s
0.200	0.213	0.00639	0,025	0.03139	0.18161	0.24439
0.400	0.427	0.01281	0,025	0.03781	0.38919	0.46481
0.600	0.635	0.01905	0,025	0.04405	0.59095	0.67905
0.800	0.859	0.02577	0,025	0.05077	0.80823	0.90977
1.000	1.103	0.03309	0,025	0.05809	1.04491	1.16109

A3.10 Calibration of probe 50

Velocity set in the tunnel	*Value measured with probe 50*	*±3.0% of reading*	*±1.0% of selected full scale range*	*Total error*	*Minimum value*	*Maximum value*
m/s	m/s	m/s	m/s	m/s	m/s	m/s
0.200	0.218	0.00654	0,025	0.03154	0.18646	0.24954
0.400	0.427	0.01281	0,025	0.03781	0.38919	0.46481
0.600	0.617	0.01851	0,025	0.04351	0.57349	0.66051
0.800	0.863	0.02589	0,025	0.05089	0.81211	0.91389
1.000	1.072	0.03216	0,025	0.05716	1.01484	1.12916

Appendix 2: Pictures.

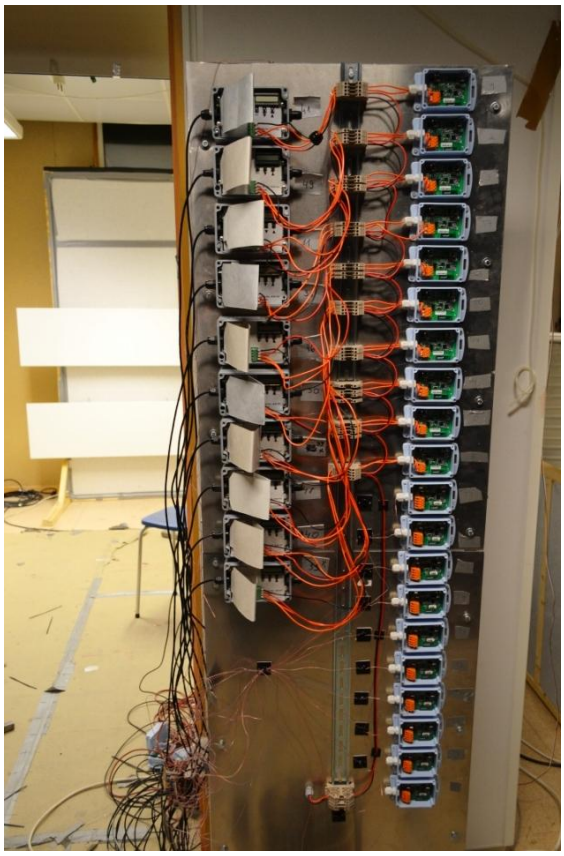

Figure 45: **WiSensys sensor platform**

Figure 46: **Air curtain system**

Figure 47: **The doorway aperture**

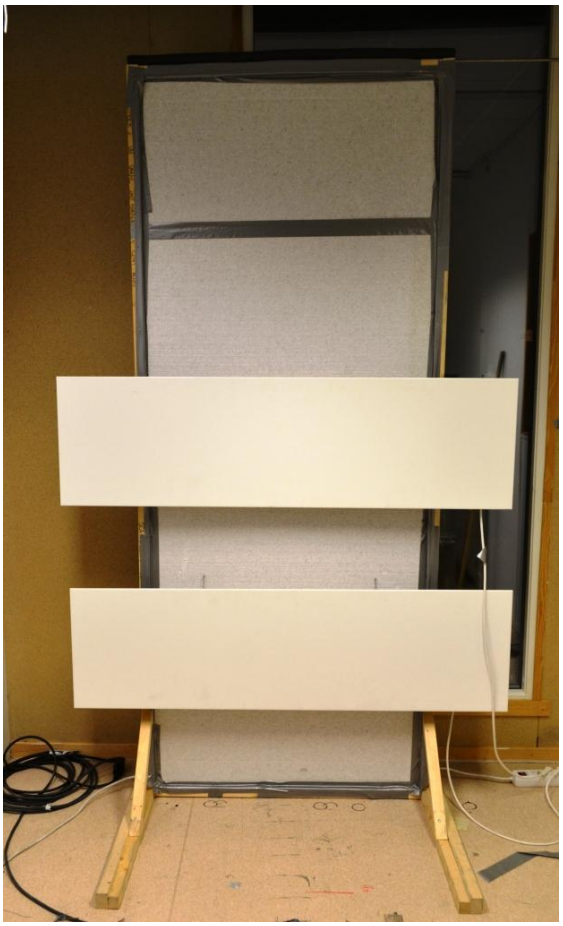

Figure 48: **Panel heaters**

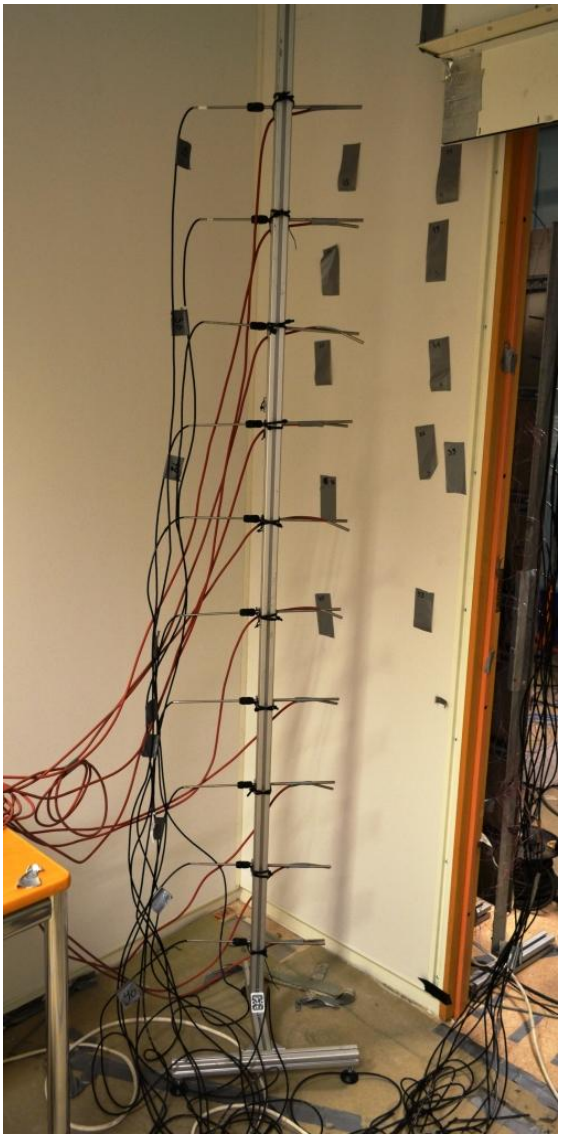

Figure 49: **The vertical pole with the probeAppendix 3. Risk analysis**

A risk analysis and procedure of running experiment was prepared before the laboratory measurements. The analysis include the following safety hazards:

- A risk of electric faults while connecting devices to the electricity plug.
- A risk of falling while mounting probes on the level near the ceiling.
- A risk of fire while the heating device is used improperly.
- A risk of fire alarm while the operation with the smoke is done inadequately.

During all laboratory operations protective goggles had to be used. All the electrical mounting had to be done with the help of laboratory technicians.

The procedure of running experiment is presented in Table X

Test of the correct operation of ventilation system:
- Startup of the fan in the indoor ventilation system supplying room air to the air curtain. - Start supplying gas in order to check if indoor ventilation system is working properly.
Measurements without indoor ventilation system:
- Connect measuring devices to the power supply. - Place anemometers and thermometers at the measuring points. - Turn on the electric heating device. - Start of measurements velocity and temperature.
Measurements with indoor ventilation system:
- Connect measuring devices to the power supply. - Place anemometers and thermometers at the measuring points. - Startup of the fan in an indoor ventilation system supplying room air to the air curtain. - Turn on the electric heating device. - Change the volume flow rate of the supplied air by changing fan rotation speed.

Appendix 4. Temperature distribution inside warm and cold zone while not using air curtain system.

	Cold zone	*Warm zone*	*Cold zone*	*Warm zone*	*Cold zone*	*Warm zone*
Height [m]	Temperature [°C]		Temperature [°C]		Temperature [°C]	
2.55	25.5	29.9	25.8	30.0	26.0	29.9
1.95	25.0	29.1	25.2	29.1	25.5	29.0
1.35	24.5	26.5	24.8	26.8	25.2	27.0
0.75	24.1	25.6	24.3	25.8	24.6	26.1
0.15	23.6	24.3	23.9	24.4	24.3	24.9

	Cold zone	*Warm zone*	*Cold zone*	*Warm zone*	*Cold zone*	*Warm zone*
Height [m]	Temperature [°C]		Temperature [°C]		Temperature [°C]	
2.55	24.4	29.3	25.7	30.4	26.5	31.2
1.95	23.3	28.5	24.5	29.7	25.4	30.5
1.35	22.5	26.8	23.6	27.9	24.5	28.8
0.75	21.9	23.1	22.9	24.1	23.8	25.0
0.15	21.4	22.2	22.4	23.0	23.2	23.9

	Cold zone	*Warm zone*	*Cold zone*	*Warm zone*	*Cold zone*	*Warm zone*
Height [m]	Temperature [°C]		Temperature [°C]		Temperature [°C]	
2.55	25.2	30.9	25.9	31.5	26.8	32.2
1.95	24.0	29.4	24.8	30.0	25.6	30.8
1.35	23.3	27.8	24.0	28.4	24.8	29.1
0.75	22.8	24.4	23.5	25.0	24.2	25.6
0.15	22.4	24.0	23.0	24.6	23.6	25.3